Published for SISSA by Springer

Received: February 23, 2018
Revised: May 14, 2018
Accepted: May 15, 2018
Published: May 28, 2018

Status of the semileptonic B decays and muon g-2 in general 2HDMs with right-handed neutrinos

Syuhei Iguro[a] **and Yuji Omura**[b]

[a] *Department of Physics, Nagoya University, Nagoya 464-8602, Japan*
[b] *Kobayashi-Maskawa Institute for the Origin of Particles and the Universe, Nagoya University, Nagoya 464-8602, Japan*

E-mail: iguro@eken.phys.nagoya-u.ac.jp, yujiomur@kmi.nagoya-u.ac.jp

Abstract: In this paper, we study the extended Standard Model (SM) with an extra Higgs doublet and right-handed neutrinos. If the symmetry to distinguish the two Higgs doublets is not assigned, flavor changing neutral currents (FCNCs) involving the scalars are predicted even at the tree level. We investigate the constraints on the FCNCs at the one-loop level, and especially study the semileptonic B meson decays, e.g. $B \to D^{(*)}\tau\nu$ and $B \to K^{(*)}ll$ processes, where the SM predictions are more than 2σ away from the experimental results. We also consider the flavor-violating couplings involving right-handed neutrinos and discuss if the parameters to explain the excesses of the semileptonic B decays can resolve the discrepancy in the anomalous muon magnetic moment. Based on the analysis, we propose the smoking-gun signals of our model at the LHC.

Keywords: Beyond Standard Model, Higgs Physics

ArXiv ePrint: 1802.01732

https://doi.org/10.1007/JHEP05(2018)173

JHEP05(2018)173

Contents

JHEP05(2018)173

1 Introduction

The Standard Model (SM) succeeds in describing almost all of the experimental results. There is one Higgs doublet to break the electroweak (EW) symmetry, and the non-vanishing vacuum expectation value (VEV) of the Higgs field generates the masses of the gauge bosons and the fermions. We do not still understand the reasons why the EW scale is around a few hundred GeV and why the couplings between the Higgs field and the fermions are so hierarchical. The Higgs particle is, however, discovered at the LHC experiment, and the signal is consistent with the SM prediction [1, 2]. Thus, we are certain that the SM describes our nature up to the EW scale.

On the other hand, it would be true that the structure of the SM is so mysterious. In addition to the mystery of the origin of the Higgs potential and couplings, the structure of the gauge symmetry is also very non-trivial. The anomaly-free conditions are miraculously satisfied: it is not easy to add extra chiral fermions to the SM. In the bottom-up approach to the new physics, one possible extension is to add extra scalars, e.g. extra Higgs doublets,

to avoid the inconsistency with the anomaly-free conditions. Such a simple extension opens up rich phenomenology, so that a simple extended SM with an extra Higgs doublet has been actually discussed since about 40 years ago [3–10].

The extended SM, besides, has other interesting aspects, from the viewpoint of the top-down approach. If we consider the new physics that can solve the mysteries of the SM, we often find extra Higgs doublets. For instance, the supersymmetric extension predicts at least one more Higgs doublet. If we consider the extended gauge symmetry, such as $SU(2)_R$, we find extra Higgs doublets that couple to the SM fermions in the effective lagrangian. If we assume that there are flavor symmetries at high energy, there would be many Higgs doublets that couple to the SM fermions flavor-dependently. Thus, it would be very interesting and important to study and summarize the predictions and the experimental constraints of the extended SM with extra Higgs doublets.

Based on this background, we investigate not only the experimental constraints but also the predictions for the observables relevant to the future experiments, in the extended SM with one Higgs doublet (2HDM). We adopt the bottom-up approach. In our model, we do not assign any symmetry to distinguish the two Higgs doublets, so that there are tree-level Flavor Changing Neutral Currents (FCNCs) involving scalars [11]. This kind of general 2HDM has been discussed, and often called the Type-III 2HDM [7–10, 12–18]. Hereafter, we abbreviate such a generic 2HDM with tree-level FCNCs as the Type-III 2HDM. We note that this kind of setup is predicted as the effective model of the extended SM with the extended gauge symmetry; e.g., the left-right symmetric model [19] and the SO(10) grand unified theory [20]. In our model, we also introduce right-handed neutrinos and allow the coupling between the right-handed neutrinos and both Higgs doublets. We simply assume that the light neutrinos are Dirac fermions, and the tiny masses are given by the small Yukawa couplings. Although the fine-tuning may be required, the Yukawa couplings between the neutrino and the extra scalars could be sizable in principle.[1]

Recently, the Type-III 2HDM is attracting a lot of attention, since it is one of the good candidates to explain the excesses reported by the BaBar, Belle, and LHCb collaborations. In the experiments, the semileptonic B decays, $B \to D^{(*)}\tau\nu$, have been measured and the results largely deviate from the SM predictions [21–28]. The B decays in the Type-III 2HDM have been studied in refs. [29–42]. Although we recently find that the explanation of $B \to D^*\tau\nu$ contradicts the leptonic B_c decay [43, 44], the Type-III 2HDM is still one of the plausible and attractive candidates to achieve the explanation of the excess in $B \to D\tau\nu$ [37]. In addition, another semileptonic B decay, i.e. $B \to K^{(*)}\mu\mu$, is also discussed recently in the 2HDM [38–40]. In the process, the LHCb collaboration has reported the deviations from the SM predictions in the measurements concerned with the angular observables [45, 46] and the lepton universality [47, 48]. Moreover, it is known that the Type-III 2HDM can accomplish the explanation of the anomalous muon magnetic moment ($(g-2)_\mu$) deviated from the SM prediction [49, 50].

[1] We note that the right-handed neutrino can have the Majorana mass term. Our discussion, however, does not change, as far as the Majorana mass is small and it is irrelevant to the active neutrino.

JHEP05(2018)173

In fact, the each explanation is elaborately achieved by tuning some proper parameters, since the experimental constraints are very strong in all cases. There are many parameters in the Type-III 2HDM, so that it may be possible to find a parameter set to explain the all excesses. In this paper, we discuss the compatibility between each of the explanations. Compared to the previous works [37–40], we take into consideration the constraint from the lepton universality of $B \to D^{(*)} l\nu$ ($l = e,\ \mu$). The compatibility of those excesses in the B decays with the $(g-2)_\mu$ discrepancy has not been also studied before. We also consider the contributions of the flavor violating couplings involving the right-handed neutrinos.

This paper is organized as follows. In section 2, we introduce our model and the simplified setup to evade the strong experimental constraints. In section 3, we summarize the experimental constraints on our model and discuss (semi)leptonic B decays in the Type-III 2HDM in section 4. We also propose our signals at the LHC in section 5. Section 6 is devoted to the summary.

2 Type-III 2HDM

We introduce the Type-III 2HDM with right-handed neutrinos. There are two Higgs doublets in our model. When the Higgs fields are written in the basis where only one Higgs doublet obtains the nonzero VEV, the fields can be decomposed as [51]

$$H_1 = \begin{pmatrix} G^+ \\ \frac{v+\phi_1+iG}{\sqrt{2}} \end{pmatrix}, \quad H_2 = \begin{pmatrix} H^+ \\ \frac{\phi_2+iA}{\sqrt{2}} \end{pmatrix}, \tag{2.1}$$

where G^+ and G are Nambu-Goldstone bosons, and H^+ and A are a charged Higgs boson and a CP-odd Higgs boson, respectively. v is the VEV: $v \simeq 246\,\mathrm{GeV}$. In this base, we write down the Yukawa couplings with the SM fermions. In the mass basis of the fermions, the Yukawa interactions are expressed by [51]

$$\begin{aligned} \mathcal{L} = &-\bar{Q}^i_L H_1 y^i_d d^i_R - \bar{Q}^i_L H_2 \rho^{ij}_d d^j_R - \bar{Q}^i_L (V^\dagger)^{ij} \widetilde{H}_1 y^j_u u^j_R - \bar{Q}^i_L (V^\dagger)^{ij} \widetilde{H}_2 \rho^{jk}_u u^k_R \\ &- \bar{L}^i_L H_1 y^i_e e^i_R - \bar{L}^i_L H_2 \rho^{ij}_e e^j_R - \bar{L}^i_L (V_\nu)^{ij} \widetilde{H}_1 y^j_\nu \nu^i_R - \bar{L}^i_L (V_\nu)^{ij} \widetilde{H}_2 \rho^{jk}_\nu \nu^k_R, \end{aligned} \tag{2.2}$$

where i, j and k represent flavor indices, and $Q = (V^\dagger u_L, d_L)^T$, $L_L = (V_\nu \nu_L, e_L)^T$ are defined. $\widetilde{H}_{1,2}$ denote $\widetilde{H}_{1,2} = i\tau_2 H^*_{1,2}$, where τ_2 is the Pauli matrix. V is the Cabbibo-Kobayashi-Maskawa (CKM) matrix and V_ν is the Maki-Nakagawa-Sakata (MNS) matrix. Fermions ($f_L,\ f_R$) ($f = u,\ d,\ e,\ \nu$) are mass eigenstates, and $y^f_i = \sqrt{2} m_{f_i}/v$, where m_{f_i} denote the fermion masses, are defined. ρ^{ij}_f are the Yukawa couplings that are independent of the SM fermion mass matrices.

There are three types of the scalars: the charged Higgs ($H^\pm$), the CP-odd scalar (A) and the two CP-even scalars ($\phi_{1,2}$). The CP-even scalars are not mass eigenstates, although the mixing should be tiny not to disturb the SM prediction. The mixing is defined as

$$\begin{pmatrix} \phi_1 \\ \phi_2 \end{pmatrix} = \begin{pmatrix} \cos\theta_{\beta\alpha} & \sin\theta_{\beta\alpha} \\ -\sin\theta_{\beta\alpha} & \cos\theta_{\beta\alpha} \end{pmatrix} \begin{pmatrix} h \\ H \end{pmatrix}. \tag{2.3}$$

JHEP05(2018)173

The masses of the heavy scalars can be evaluated as

$$m_H^2 \simeq m_A^2 + \lambda_5 v^2, \tag{2.4}$$

$$m_{H^\pm}^2 \simeq m_A^2 - \frac{\lambda_4 - \lambda_5}{2} v^2. \tag{2.5}$$

m_H, m_A and m_{H^+} denote the masses of the heavy CP-even, CP-odd and charged Higgs scalars. λ_4 and λ_5 are the dimensionless couplings in the Higgs potential: $V(H_i) = \lambda_4 (H_1^\dagger H_2)(H_2^\dagger H_1) + \frac{\lambda_5}{2}(H_1^\dagger H_2)^2 + \ldots$ The mass differences are relevant to the electro-weak precision observables (EWPOs) and the explanation of the $(g-2)_\mu$ anomaly [49, 50].

2.1 Setup of the texture

ρ_f are 3×3 matrices and the each element is the free parameter that is constrained by the flavor physics and the collider experiments. The comprehensive study about the phenomenology in the Type-III 2HDM has been done in ref. [32]. There are many choices for the matrix alignment, but actually only a few elements are allowed to be sizable according to the stringent experimental bounds [32].

First, let us discuss the physics concerned with ρ_u and ρ_d. The all off-diagonal elements of ρ_d are strongly constrained by the $\Delta F = 2$ processes. ρ_u^{uc} and ρ_u^{cu} have to be small to avoid the stringent constraint that comes from the D-$\overline{D}$ mixing. Besides, we find that the size of the Yukawa coupling involving the light quarks are limited by the direct search at the collider experiments. Even ρ_u^{ut} and ρ_u^{tu} may be constrained by the bounds from the collider experiment, e.g., the upper limit from the same-sign top signal.[2] Moreover, ρ_u^{ut} and ρ_u^{tu} are strongly constrained by the K-$\overline{K}$ mixing at the one-loop level. Thus, it is difficult to expect that the couplings between the light quarks (u, d, s) and the other quarks are larger than $\mathcal{O}(0.01)$. The diagonal elements, on the other hand, could be $\mathcal{O}(0.1)$, unless the off-diagonal elements are not sizable [54].

Based on the examination, we consider the case that $|\rho_u^{ct}|$ and/or $|\rho_u^{tc}|$ are sizable. One of our motivations of this study is to investigate the compatibility among the explanations of the excesses in the Type-III 2HDM. It is pointed out that the sizable ρ_u^{tc} can improve the discrepancies in the $b \to sll$ and $b \to cl\nu$ processes [37]. Eventually, we consider the following simple textures of ρ_f from the phenomenological point of view:

$$\rho_u \simeq \begin{pmatrix} 0 & 0 & 0 \\ 0 & 0 & \rho_u^{ct} \\ 0 & \rho_u^{tc} & \rho_u^{tt} \end{pmatrix}, \quad |\rho_d^{ij}| \ll \mathcal{O}(0.1). \tag{2.6}$$

The other elements of ρ_u are assumed to be at most $\mathcal{O}(0.01)$, so that the physics involving ρ_u^{ct}, ρ_u^{tc}, and ρ_u^{tt} is mainly discussed in this paper. Note that we ignore all elements of ρ_d and assume that all sizable Yukawa couplings are real, through our paper.

Next, we discuss the Yukawa couplings with leptons. We can also find the strong upper bounds on the Yukawa couplings in the lepton sector. The lepton flavor violating (LFV)

[2] Note that there is a way to avoid the strong constraint, considering the degenerate masses of the scalars [52, 53].

JHEP05(2018)173

processes are predicted by the neutral scalar exchanging, if the off-diagonal elements of ρ_e are sizable. In the case that the extra Yukawa couplings involving electron are large, the LEP experiment can easily exclude our model. Interestingly, the authors of refs. [49, 50] have pointed out that the large $\rho_e^{\mu\tau}$ and $\rho_e^{\tau\mu}$ can achieve the explanation of the $(g-2)_\mu$, that is largely deviated from the SM prediction. The explanation, however, requires the other Yukawa couplings to be small [49, 50]. Then, we especially consider the following texture of ρ_e:

$$\rho_e \simeq \begin{pmatrix} 0 & 0 & 0 \\ 0 & 0 & \rho_e^{\mu\tau} \\ 0 & \rho_e^{\tau\mu} & 0 \end{pmatrix}. \tag{2.7}$$

Note that the diagonal elements, $\rho_e^{\tau\tau}$ and $\rho_e^{\mu\mu}$, are also strongly constrained, as far as $\rho_e^{\mu\tau}$ and $\rho_e^{\tau\mu}$ are sizable [50].

In our study, we also consider the contribution of ρ_ν to flavor physics. This investigation has not been done well in the type-III 2HDM. This is because the tiny Dirac neutrino masses predict small Yukawa couplings so that ρ_ν is also naively expected to be small. ρ_ν, however, does not contribute to the active neutrino masses, directly. If both ρ_ν and ρ_e are sizable, ρ_ν would contribute to the neutrino masses radiatively. Otherwise, ρ_ν could be large compared to y_ν^i, in the bottom-up approach. The unique texture as in eq. (2.7) may also allow ρ_ν to be sizable. Based on this consideration, we study the upper bound on ρ_ν and discuss the impact on the physical observables in flavor physics.

3 The summary of the experimental constraints

In this section, we discuss the physics triggered by the Yukawa couplings in eq. (2.6) and eq. (2.7). The contribution of ρ_ν is also studied. Note that we are interested in the light scalar scenario. In order to avoid the exotic decay, e.g. $t \to Hc$, and enlarge the new physics contributions maximumly, the extra scalar masses are set to 200 GeV or 250 GeV below.

3.1 The experimental constraints on ρ_u

To begin with, we summarize the experimental constraints on ρ_u. In our study, the texture of ρ_u is approximately given by eq. (2.6). Then, we can evade the strong bound from the $\Delta F = 2$ processes at the tree level. The measurements of the meson mixings are, however, very sensitive to new physics contributions, so that we need to study the bounds carefully, taking into account the loop corrections.

In our setup, the one-loop corrections involving the charged Higgs and the W-boson, that are described in figure 1, contribute to the B-$\overline{B}$ mixing and the B_s-$\overline{B_s}$ mixing. The operators induced by the one-loop corrections are

$$\mathcal{H}_{\rm eff}^{\Delta F=2} = -C_{LL}^q (\bar{q}\gamma^\mu P_L b)(\bar{q}\gamma_\mu P_L b), \tag{3.1}$$

JHEP05(2018)173

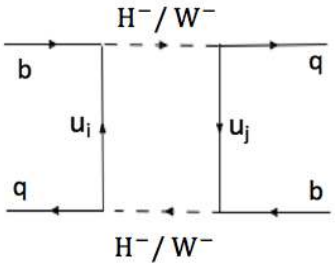

Figure 1. The diagrams that contribute to the $B_{(s)}$-$\overline{B_{(s)}}$ mixing.

where $q = s,\ d$. The new physics contribution to the coefficient, C_{LL}, is evaluated at the one-loop level as

$$C_{LL}^{q} = \frac{1}{128\pi^2 m_{H^+}^2}\sum_{k,l}(V^\dagger\rho_u)^{qk}(\rho_u^\dagger V)^{lb}\left[(\rho_u^\dagger V)^{kb}(V^\dagger\rho_u)^{ql}G_1(x_k,x_l)\right.$$
$$\left.-\frac{4g^2 m_{u_k}m_{u_l}}{m_{H^+}^2}V_{kb}V_{lq}^* G_2(x_k,x_l,x_W)+\frac{g^2 m_{u_k}m_{u_l}}{m_W^2}V_{kb}V_{lq}^* G_3(x_k,x_l,x_W)\right], \tag{3.2}$$

where $x_k = m_{u_k}^2/m_{H^+}^2$ and $x_W = m_W^2/m_{H^+}^2$. The functions G_i $(i = 1, 2, 3)$ are defined as

$$G_1(x,y) = \frac{1}{x-y}\left[\frac{x^2\log x}{(1-x)^2}+\frac{1}{1-x}-\frac{y^2\log y}{(1-y)^2}-\frac{1}{1-y}\right], \tag{3.3}$$

$$G_2(x,y,z) = -\frac{1}{(x-y)(1-z)}\left[\frac{x\log x}{1-x}-\frac{y\log y}{1-y}-\frac{x\log\frac{x}{z}}{z-x}+\frac{y\log\frac{y}{z}}{z-y}\right], \tag{3.4}$$

$$G_3(x,y,z) = -\frac{1}{x-y}\left[\frac{1}{1-z}\left(\frac{x\log x}{1-x}-\frac{y\log y}{1-y}\right)-\frac{z}{1-z}\left(\frac{x\log\frac{x}{z}}{z-x}-\frac{y\log\frac{y}{z}}{z-y}\right)\right]. \tag{3.5}$$

Using the coefficient, the mass difference, $\Delta m_{B_{d,s}}$, can be evaluated as

$$\Delta m_{B_{d_i}} = -2\mathrm{Re}(C_{LL}^q)\frac{m_{B_{d_i}}F_{B_{d_i}}^2 B_{B_{d_i}}}{3}, \tag{3.6}$$

where $m_{B_{d_i}}$, $F_{B_{d_i}}$ and $B_{B_{d_I}}$ are a mass, a decay constant and the bag parameter of B_{d_i} meson, respectively. We note that C_{LL}^q includes the SM correction.

The deviations of the neutral $B_{(s)}$ meson mixing will be evaluated including the SM corrections, but it is certain that there are non-negligible uncertainties in the theoretical predictions. In our analysis, we calculate our predictions, using the input parameters in appendix A. In order to draw the constraints on the Yukawa couplings, we require that the deviations induced by the charged Higgs contributions are within the 2σ errors of the SM predictions and the experimental results. We simply adopt the SM predictions ($\Delta M_{B_{(s)}}^{\mathrm{SM}}$) given by ref. [55]: $0.45\ [\mathrm{ps}^{-1}] \leq \Delta M_B^{\mathrm{SM}} \leq 0.78\ [\mathrm{ps}^{-1}]$ and $16.2\ [\mathrm{ps}^{-1}] \leq \Delta M_{B_s}^{\mathrm{SM}} \leq 21.9$ (95% CL). Then, we define $\delta(\Delta M_{B_{(s)}}) = \Delta M_{B_{(s)}}^{\mathrm{exp}} - \Delta M_{B_{(s)}}^{\mathrm{SM}}$, where $\Delta M_{B_{(s)}}^{\mathrm{exp}}$ are the experimental values: $\Delta M_B^{\mathrm{exp}} = 0.5064 \pm 0.0019\ [\mathrm{ps}^{-1}]$ and $\Delta M_{B_s}^{\mathrm{exp}} = 17.757 \pm 0.021\ [\mathrm{ps}^{-1}]$ [56]. Taking into account the 2σ uncertainties, $\delta(\Delta M_{B_{(s)}})$ are within the following ranges:

$$-0.27 \leq \delta(\Delta M_B)[\mathrm{ps}^{-1}] \leq 0.06, \quad -4.1 \leq \delta(\Delta M_{B_s})[\mathrm{ps}^{-1}] \leq 1.6. \tag{3.7}$$

JHEP05(2018)173

$B-\overline{B}$ Mixing			
$m_{H^\pm}$	$\lvert\rho_u^{ct}\rvert$	$\lvert\rho_u^{tc}\rvert$	$\lvert\rho_u^{tt}\rvert$
200 [GeV]	0.307	1.00	0.741
250 [GeV]	0.340	1.12	0.814
$B_s-\overline{B_s}$ Mixing			
$m_{H^\pm}$	$\lvert\rho_u^{ct}\rvert$	$\lvert\rho_u^{tc}\rvert$	$\lvert\rho_u^{tt}\rvert$
200 [GeV]	0.276	0.748	0.428
250 [GeV]	0.307	0.836	0.473

Table 1. The upper bounds on the up-type Yukawa couplings from the $\Delta F = 2$ processes, fixing $m_{H^\pm}$ at $m_{H^\pm} = 200\,\text{GeV}$ and $250\,\text{GeV}$.

If the magnitudes of the Yukawa couplings are below the upper bounds in table 1 when $m_{H^\pm} = 200\,\text{GeV}$ and $250\,\text{GeV}$, the charged Higgs contributions are within these ranges in eq. (3.7). The results in table 1 are consistent with the ones in ref. [57].

Next, we consider the rare decays of the mesons, such as $B \to X_s\gamma$. The $b \to s$ transition is given by the C_7 operator, according to the diagram in figure 2,

$$\mathcal{H}_{\text{eff}}^{b\to s\gamma} = -\frac{4G_F}{\sqrt{2}} V_{tb}V_{ts}^* \frac{e}{16\pi^2} m_b C_7 F^{\mu\nu}(\overline{s_L}\sigma_{\mu\nu}b_R) + h.c., \tag{3.8}$$

where C_7 in our model is evaluated at the one-loop level as follows:

$$C_7 = \frac{1}{4\sqrt{2}G_F m_{H^+}^2 V_{tb}V_{ts}^*} \sum_i (V^\dagger \rho_u)^{si}(\rho_u^\dagger V)^{ib} \left[\frac{2}{3}G_1^7(x_i) + G_2^7(x_i)\right]. \tag{3.9}$$

$G_1^7(x)$ and $G_2^7(x)$ are defined as

$$G_1^7(x) = -\frac{2+3x-6x^2+x^3+6x\log x}{12(1-x)^4}, \tag{3.10}$$

$$G_2^7(x) = -\frac{1-6x+3x^2+2x^3-6x^2\log x}{12(1-x)^4}. \tag{3.11}$$

The $b \to s\gamma$ has been experimentally measured and the result is consistent with the SM prediction [58]. Then, this process becomes a stringent bound on our model. For instance, the size of C_7 at the bottom quark mass scale should be within the range, $-0.055 \leq C_7(m_b) \leq 0.02$, according to the global fitting [34].

In table 2, we derive the upper bounds on the up-type Yukawa couplings using the value in ref. [34]. The charged Higgs mass, $m_{H^\pm}$, is fixed at $m_{H^\pm} = 200\,\text{GeV}$ or $250\,\text{GeV}$. These results are consistent with the ones derived from the values in refs. [56, 59].

JHEP05(2018)173

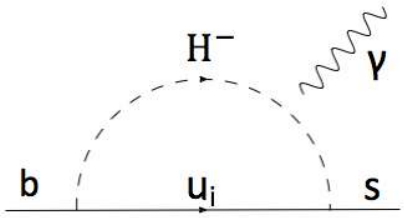

Figure 2. The diagram that contributes to the $b \to s\gamma$ process.

$m_{H^\pm}$	$\lvert\rho_u^{ct}\rvert$	$\lvert\rho_u^{tc}\rvert$	$\lvert\rho_u^{tt}\rvert$
200 [GeV]	1.03	1.07	1.71
250 [GeV]	1.17	1.33	1.94

Table 2. The upper bounds from the global fitting: $-0.055 \leq \Delta C_7(m_b) \leq 0.02$. m_{H^+} is fixed at $m_{H^\pm} = 200\,\text{GeV}$ and $250\,\text{GeV}$, respectively.

In addition, we could obtain the limits on the Yukawa couplings from the direct search for the flavor-violating processes. In our model, the flavor-violating top quark decay is predicted as

$$\begin{aligned} BR(\text{t} \to \text{hc}) &= \frac{|\rho_u^{tc}|^2 + |\rho_u^{ct}|^2}{64\pi\Gamma_t} \cos^2\theta_{\beta\alpha} \left(1 - \frac{m_h^2}{m_t^2}\right) \\ &= 9.7 \times 10^{-4} \ \left(|\rho_u^{tc}|^2 + |\rho_u^{ct}|^2\right) \left(\frac{\cos\theta_{\beta\alpha}}{0.1}\right)^2, \end{aligned} \tag{3.12}$$

where Γ_t is defined as $\Gamma_t = 1.41\,\text{GeV}$. Based on the results in refs. [60–62], we derive the following upper bound:

$$|\cos\theta_{\beta\alpha}| \times \sqrt{|\rho_u^{tc}|^2 + |\rho_u^{ct}|^2} \leq 9.1 \times 10^{-2}. \tag{3.13}$$

In our study, we survey the parameter region with $\mathcal{O}(1)$ ρ_u^{tc} and/or ρ_u^{ct}. In addition, $\rho_e^{\mu\tau}$ and $\rho_e^{\tau\mu}$ are large in some cases. As we discuss below, the flavor-violating Higgs decay, such as $h \to \mu\tau$, also significantly constraints $\cos\theta_{\beta\alpha}$. Then, we simply assume that $|\cos\theta_{\beta\alpha}|$ is at most $\mathcal{O}(10^{-3})$ and ignore the corrections that depend on $\cos\theta_{\beta\alpha}$.

3.2 The experimental constraints on ρ_e and ρ_ν

In this section, we summarize the constraints on ρ_e and ρ_ν. Interestingly, the texture of ρ_e in eq. (2.7) can evade the strong experimental bounds from the LFV processes. On the other hand, the discrepancy of $(g-2)_\mu$ can be resolved by the sizable (μ, τ) Yukawa couplings [49, 50].

Let us discuss the tree-level contributions to the physical observables, that are given by $\rho_e^{\mu\tau}$, $\rho_e^{\tau\mu}$ and ρ_ν. In the type-III 2HDM, the charged Higgs boson exchanging induces $\tau \to l\nu\overline{\nu}$ $(l = \mu, e)$ at the tree level. We define the following observable:

$$\left(\frac{g_\mu}{g_e}\right)^2 \equiv \frac{BR(\tau \to \mu\nu\overline{\nu})/f(y_\mu)}{BR(\tau \to e\nu\overline{\nu})/f(y_e)}, \tag{3.14}$$

JHEP05(2018)173

where $y_l \equiv m_l^2/m_\tau^2$ $(l = e, \mu, \tau)$ are defined and $f(y)$ is a phase space function. This measurement has been experimentally given as $g_\mu/g_e = 1.0018 \pm 0.0014$ [63]. In our model, the extra contribution to the each branching ratio of $l_1 \to l_2\nu\nu$ decay is proportional to

$$|g^\nu_{l_1 l_2}|^2 \equiv \sum_{ij} \left|(\widetilde{\rho}_\nu)^{l_2 i}\right|^2 \left|(\widetilde{\rho}_\nu)^{l_1 j}\right|^2, \ |g^e_{l_1 l_2}|^2 \equiv \sum_{ij} \left|\left(V_\nu^\dagger \rho_e\right)^{i l_2}\right|^2 \left|\left(V_\nu^\dagger \rho_e\right)^{j l_1}\right|^2, \tag{3.15}$$

where $\widetilde{\rho}_\nu$ is defined as $\widetilde{\rho}_\nu \equiv V_\nu \rho_\nu$. Allowing the 2σ deviation of g_μ/g_e, we obtain the upper bounds on the Yukawa couplings at $m_{H^\pm} = 200(250)$ GeV as follows:

$$|g^\nu_{\mu\tau}| \leq 0.25\,(0.4), \ |g^e_{\mu\tau}| \leq 0.25\,(0.4). \tag{3.16}$$

Next, we study the constraints from the michel parameter of the lepton decays. As discussed above, the charged Higgs exchanging contributes to $l_1 \to l_2\nu\bar{\nu}$ decays. The constraints derived from the michel parameters are summarized in ref. [63]. Following ref. [63], we derive the bounds on ρ_ν and ρ_e as

$$\left|0.76 \times g^\nu_{l_1 l_2} \left(\frac{200}{m_{H^\pm}}\right)^2\right| \leq c^\nu_{l_1 l_2} \tag{3.17}$$

and

$$\left|0.76 \times g^e_{l_1 l_2} \left(\frac{200}{m_{H^\pm}}\right)^2\right| \leq c^e_{l_1 l_2}. \tag{3.18}$$

$c^\nu_{l_1 l_2}$ and $c^e_{l_1 l_2}$ are the upper bounds from $l_1 \to l_2\nu\nu$, introduced in ref. [63]: $(c^\nu_{\mu e}, c^\nu_{\tau e}, c^\nu_{\tau\mu}) = (0.55, 2.01, 2.01)$ and $(c^e_{\mu e}, c^e_{\tau e}, c^e_{\tau\mu}) = (0.035, 0.70, 0.72)$. Thus, we obtain the strong bounds on $g^\nu_{\mu e}$ and $g^e_{\mu e}$: $|g^\nu_{\mu e}| \leq 0.73(1.13)$ and $|g^e_{\mu e}| \leq 0.046(0.072)$ at $m_{H^\pm} = 200(250)$ GeV. The other elements, on the other hand, can be $\mathcal{O}(1)$.

Note that in our texture as eq. (2.7), $\rho_e^{\mu\mu}$ and ρ_e^{ee} are assumed to be vanishing, so that the stringent constraints from the LFV decays of the charged leptons can be evaded. In our setup with ρ_e in eq. (2.7), the scalar mixing, $\cos\theta_{\beta\alpha}$, enhances the LFV τ decay, $\tau \to 3\mu$, according to the neutral scalar exchanging. In order to avoid the current experimental bound, $Br(\tau \to 3\mu) < 2.1 \times 10^{-8}$ [63], we obtain the bound as

$$|\cos\theta_{\beta\alpha}| \times \overline{\rho_e^{\mu\tau}} \lesssim 0.168 \times \left(1 - \frac{(125\,\mathrm{GeV})^2}{m_H^2}\right)^{-1}, \tag{3.19}$$

where $\overline{\rho_e^{\mu\tau}} \equiv \sqrt{|\rho_e^{\mu\tau}|^2 + |\rho_e^{\tau\mu}|^2}$ is defined. Then we can conclude that the (μ, τ) elements of ρ_e can be larger than $\mathcal{O}(0.1)$ when $|\cos\theta_{\beta\alpha}|$ is suppressed. In the case that $\rho_e^{\mu\mu}$ and ρ_e^{ee} are sizable, the upper bounds on the parameters are estimated as $\mathcal{O}(10^{-4})$ when the CP even scalar mass is $\mathcal{O}(100)$ GeV and $\overline{\rho_e^{\mu\tau}}$ is $\mathcal{O}(1)$ [50].

We can derive the constraint from the flavor-violating decay of 125 GeV neutral scalar. In our model, the branching ratio of the decay to two fermions (f_i, f_j) is given by

$$\begin{aligned} BR(h \to f_i f_j) &= \frac{\Gamma(h \to f_i \bar{f}_j) + \Gamma(h \to \bar{f}_i f_j)}{\Gamma_h} \\ &= \frac{\cos^2\theta_{\beta\alpha} \left(|\rho_f^{ij}|^2 + |\rho_f^{ji}|^2\right) m_h}{16\pi\Gamma_h}, \end{aligned} \tag{3.20}$$

JHEP05(2018)173

	$\Delta_{\mu\tau}$	$\Delta_{e\tau}$	$\Delta_{e\mu}$
$m_{H^\pm}$=200 [GeV]	0.135	0.116	0.173×10^{-3}
$m_{H^\pm}$=250 [GeV]	0.211	0.181	0.275×10^{-3}

Table 3. The upper bounds on $\widetilde{\rho_\nu} = V_\nu \rho_\nu$ at 90% CL in the cases with $m_{H^\pm} = 200\,\text{GeV}$ and 250 GeV. $\Delta_{ll'} = \sum_j |(\widetilde{\rho_\nu})^{lj}(\widetilde{\rho_\nu})^{l'j*}|$ is defined.

where Γ_h is the total decay width of h whose mass is around 125 GeV and fixed at $\Gamma_h = 4.1\,\text{MeV}$. Following the upper bound on $BR(h \to \mu\tau)$ [64–66], we find the upper limit on the μ-τ coupling at 2σ:

$$|\cos\theta_{\beta\alpha}| \times \overline{\rho_e^{\mu\tau}} \leq 2.3 \times 10^{-3}. \tag{3.21}$$

Thus, we obtain the strong bound on $\cos\theta_{\beta\alpha}$. As mentioned above, $|\cos\theta_{\beta\alpha}|$ is assumed to be at most $\mathcal{O}(10^{-3})$ and the contributions to the flavor physics are ignored in our analysis.

We consider the one-loop contributions to the LFV process and the Z-boson decay. The correction involving only ρ_e is summarized in ref. [50]. Assuming that the all elements of ρ_e are vanishing, we derive the constraints on ρ_ν from the LFV processes. The upper bounds from $l' \to l\gamma$ are summarized in table 3. $\Delta_{ll'}$ is defined as $\Delta_{ll'} = \sum_j |(\widetilde{\rho_\nu})^{lj}(\widetilde{\rho_\nu})^{l'j*}|$. As we see in table 3, $\Delta_{e\mu}$ is strongly constrained, while the other elements can be large.

In addition, the decay of the Z boson may be largely deviated from the SM prediction, according to the extra scalars, at the one-loop level. In our work, we consider the case that either ρ_e or ρ_ν is sizable. Then, the contribution to the Z boson decay through the penguin diagrams is suppressed. We have calculated the deviation of $BR(Z \to \nu\bar{\nu})$, but it is not so large. We find that the upper bounds on $\left|\overline{\rho_e^{\mu\tau}}\right|$ and $|\overline{\rho_\nu}|$ can reach $\mathcal{O}(1)$, even if the deviation of $BR(Z \to \nu\bar{\nu})$ is required to be within 2σ.

Note that ρ_ν would be strongly constrained by the cosmological observation, depending on the mass spectrum of the right-handed neutrino. We comment on the bound in section 4.3.3.

4 The (semi)leptonic B decays

Based on the studies in section 3, we investigate the impact of our Type-III 2HDM on the (semi)leptonic B-meson decays. As discussed in refs. [35, 37, 38], the 2HDMs potentially have a great impact on $B \to D^{(*)}l\nu$ and $B \to K^{(*)}ll$ processes ($l = e, \mu, \tau$), where the discrepancies between the experimental results and the SM predictions are reported. In particular, the global analyses on $B \to K^{(*)}ll$ suggest that C_9 and C_{10} operators may be deviated from the SM values. Besides, the flavor universality of $B \to K^{(*)}ll$ is also inconsistent with the SM prediction in the experimental results. In our model, ρ_ν can contribute to the C_9 and C_{10} operators, flavor-dependently. Thus, it becomes very important to find how well the tension can be relaxed, taking into account the ρ_ν contribution.

JHEP05(2018)173

4.1 The bounds from the $B \to l\nu$ decays

First, we discuss the leptonic decays of the B meson: $B \to l\nu$. In our model, the charged Higgs exchanging contributes to the B meson decays as

$$\mathcal{H}^l_{B_q} = -\frac{\rho_e^{l'l}\rho_u^{tq}}{m^2_{H^\pm}}(V_\nu^*)_{l'j}V_{tb}(\overline{\nu_L^j}l_R)(\overline{b_L}q_R) - \frac{(\widetilde{\rho_\nu})^{lj*}\rho_u^{tq}}{m^2_{H^\pm}}V_{tb}(\overline{\nu_R^j}l_L)(\overline{b_L}q_R). \tag{4.1}$$

The flavor of the neutrino in the final state can not be distinguished, so that let us define the parameters,

$$|\kappa^e_{lq}|^2 \equiv \sum_j \left|\rho_e^{jl}\rho_u^{tq}\right|^2, \ |\kappa^\nu_{lq}|^2 \equiv \sum_j \left|(\widetilde{\rho_\nu})^{lj*}\rho_u^{tq}\right|^2, \tag{4.2}$$

and discuss the constraints on those products.

In our setup, the $(t,\ c)$-elements of ρ_u are sizable, so that the leptonic decay of B_c is deviated from the SM prediction. The leptonic decay has not been measured by any experiments, but we can derive the constraint from the total decay width of B_c [43] and the measurement at the LEP experiment [44]. Adopting the severe constraint, $BR(B_c \to \tau\nu) \leq 10\%$ [44], we obtain the upper bounds on the lepton Yukawa couplings as follows:

$$|\kappa^{e,\nu}_{\tau c}| \times \left(\frac{200\,\mathrm{GeV}}{m_{H^\pm}}\right)^2 \leq 0.025. \tag{4.3}$$

In our assumption, the $(t,\ u)$ elements are less than $\mathcal{O}(0.01)$. Even in such a case, the sizable $\rho_e^{\mu\tau,\tau\mu}$ and ρ_ν may largely contribute the B_u decays. The contributions to $B_u \to l\bar{\nu}$ are linear to $|\kappa^e_{lu}|^2$ and $|\kappa^\nu_{lu}|^2$. These products at $m_{H^\pm} = 200(250)\,\mathrm{GeV}$ are constrained by the leptonic B_u decays as

$$|\kappa^{e,\nu}_{\mu u}| \leq 0.99 \times 10^{-4}\ (1.55 \times 10^{-4}), \tag{4.4}$$

$$|\kappa^{e,\nu}_{\tau u}| \leq 1.18 \times 10^{-3}\ (1.84 \times 10^{-3}). \tag{4.5}$$

We could also derive the bound from $B_s \to \mu\mu$. The error of the experimental measurement is still so large that it is difficult to draw a stringent bound on our model. The branching ratio of this rare decay, however, relates to the semi-leptonic B decay, $B \to K^{(*)}\mu\mu$, so that we give a discussion about this process below.

4.2 $B \to D^{(*)}l\nu$ $(l = e,\ \mu,\ \tau)$

We investigate the constraints from the semileptonic B decay; e.g., $B \to D^{(*)}l\nu$ $(l = e, \mu, \tau)$. There is a discrepancy in $B \to D^{(*)}\tau\nu$, although $B \to D^{(*)}e\nu$ and $B \to D^{(*)}\mu\nu$ are consistent with the SM predictions. In our model, the charged Higgs exchanging flavor-dependently contributes to these processes via ρ_e and ρ_u couplings, as shown in eq. (4.1). Then, the discrepancy of $B \to D^{(*)}\tau\nu$ could be ameliorated by the contribution of the diagram in figure 3 [37], although the flavor universality of $B \to D^{(*)}l\nu$ $(l = e,\ \mu)$ may constrain our setup strongly. We define the observables to measure the universality as follow:

$$R(D^{(*)})_{e\mu} = \frac{BR(B \to D^{(*)}e\bar{\nu})}{BR(B \to D^{(*)}\mu\bar{\nu})}. \tag{4.6}$$

JHEP05(2018)173

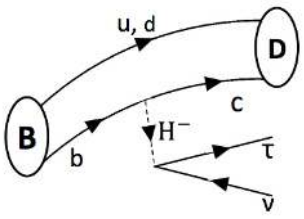

Figure 3. Diagram that contributes to the $B \to D\tau\nu$.

	$m_{H^\pm}$	$R(D^{(*)})_{e\mu} = 0.95$	$R(D^{(*)})_{e\mu} = 0.98$
D^*	200 [GeV]	5.16×10^{-2}	0.34×10^{-1}
D^*	250 [GeV]	8.06×10^{-2}	5.32×10^{-2}
D	200 [GeV]	1.08×10^{-2}	0.70×10^{-2}
D	250 [GeV]	1.68×10^{-2}	1.08×10^{-2}

Table 4. The upper bounds on $|\kappa^{e,\nu}_{\mu c}|$ from the lepton universality of $B \to D^{(*)}l\nu$ ($l = e, \mu$). We impose the upper bounds on $R(D^{(*)})_{e\mu}$ as $R(D^{(*)})_{e\mu} > 0.95$ and $R(D^{(*)})_{e\mu} > 0.98$ [67]. The process, $B \to D^*(D)l\nu$, is labeled as D^* (D) on the first column.

The deviations should not exceed a few percent: $R(D^*)_{e\mu} = 1.04 \pm 0.05 \pm 0.01$ [67]. Fixing the charged Higgs mass at $m_{H^\pm} = 200(250)\,\text{GeV}$, we derive the upper bounds on $\kappa^{e,\nu}_{\mu c}$. In the table 4, the upper bounds on $\kappa^{e,\nu}_{\mu c}$ with $m_{H^\pm} = 200\,\text{GeV}$ and $250\,\text{GeV}$ are summarized. The calculation is based on ref. [37]. Note that, roughly speaking, only $BR(B \to D^{(*)}\mu\bar{\nu})$ is always enhanced, so the only lower limit on $R(D^{(*)})_{e\mu}$ is shown in table 4. We impose the bounds as $R(D^{(*)})_{e\mu} > 0.95$ and $R(D^{(*)})_{e\mu} > 0.98$ [67].

The semileptonic B decay associated with τ lepton in the final state is also deviated from the SM prediction, in our model. In ref. [37], $R(D^{(*)})$ are well studied in the Type-III 2HDM with only ρ_e, ρ_d and ρ_u, and we find that at least $R(D)$ can be enhanced so much that it is consistent with the experimental result. The lowest value to achieve the world average of $R(D)$ ($R(D)$=0.407±0.046) and $R(D^*)$ ($R(D^*)$=0.304±0.015) at the 1σ level [56] is

$$|\kappa^{e,\nu}_{\tau c}| \geq 2.12 \times 10^{-2} \text{ for } R(D), \tag{4.7}$$

$$|\kappa^{e,\nu}_{\tau c}| \geq 2.89 \times 10^{-1} \text{ for } R(D^*), \tag{4.8}$$

when the charged Higgs mass is fixed at $m_{H^\pm} = 200\,\text{GeV}$. Note that our SM prediction is $R(D) = 0.299$ and $R(D^*) = 0.253$ with $\text{BR}(B_c \to \tau\nu) = 2.2\%$ in our parameter set [68]. This lowest value for $R(D)$ is very close to the upper bound from $B_c \to \tau\nu$ in eq. (4.3). We can find that the value required by $R(D^*)$ is totally excluded by the B_c decay. Besides, the lepton universality of this semileptonic decay provides the stringent bounds on $\kappa^{e,\nu}_{\mu c}$, as shown in table 4. Thus, we concluded that either $|\kappa^{e}_{\tau c}|$ or $|\kappa^{\nu}_{\tau c}|$ should be $\mathcal{O}(1) \times 10^{-2}$ to achieve the discrepancy of $R(D)$ without any conflict with the other observables concerned with the B decay. Otherwise, the anomaly of $R(D)$ cannot be resolved in our model.

JHEP05(2018)173

4.3 $B \to K^{(*)}ll$

Finally, we consider $B \to K^{(*)}ll$ in our model. In the so-called aligned 2HDM, this process has been discussed in ref. [38]. The Type-III 2HDM case with only ρ_e has also been shortly studied in ref. [37]. In our study, we include the box diagrams induced by ρ_e and ρ_ν and take into account the consistency with the explanations of $(g-2)_\mu$ and $R(D)$, that has not been done before.

In the $B \to K^{(*)}ll$ processes, there are several interesting observables where the discrepancies between the SM predictions and the experimental results are reported by the LHCb collaboration. One is P_5' that is concerned with the angular distribution of the $B \to K^*\mu\mu$ process [45, 46], and another is $R(K^*)$ [47] and $R(K)$ [48] that measure the lepton universalities of $B \to K^*\mu\mu/ee$ and $B \to K\mu\mu/ee$, respectively. The observables are governed by C_9^l and C_{10}^l operators defined as

$$\mathcal{H}^l_{B_s} = -g_{\rm SM}\left\{C_9^l(\overline{s_L}\gamma_\mu b_L)(\bar{l}\gamma^\mu l) + C_{10}^l(\overline{s_L}\gamma_\mu b_L)(\bar{l}\gamma^\mu\gamma_5 l) + h.c.\right\}, \tag{4.9}$$

where $g_{\rm SM}$ is the factor from the SM contribution:

$$g_{\rm SM} = \frac{4G_F}{\sqrt{2}}V_{tb}V_{ts}^*\frac{e^2}{16\pi^2}. \tag{4.10}$$

In our model, the Wilson coefficients C_9^l and C_{10}^l consist of the SM and the new physics contributions as $C_9^l = (C_9)_{\rm SM} + \Delta C_9^l$ and $C_{10}^l = (C_{10})_{\rm SM} + \Delta C_{10}^l$. ΔC_9^l and ΔC_{10}^l are given by

$$\begin{aligned}\Delta C_{9(l)} = {} & \frac{-1}{2\sqrt{2}G_{\rm F}m_{H^+}^2V_{tb}V_{ts}^*}\sum_i(V^\dagger\rho_u)^{si}(\rho_u^\dagger V)^{ib}\left[\frac{2}{3}G_{\gamma 1}(x_i) + G_{\gamma 2}(x_i)\right] \\ & + \frac{1}{4\pi\alpha V_{tb}V_{ts}^*}\left(-\frac{1}{2} + 2s_W^2\right)\sum_i(V^\dagger\rho_u)^{si}(\rho_u^\dagger V)^{ib}G_Z(x_i),\end{aligned} \tag{4.11}$$

$$\Delta C_{10(l)} = \frac{1}{4\pi\alpha V_{tb}V_{ts}^*}\frac{1}{2}\sum_i(V^\dagger\rho_u)^{si}(\rho_u^\dagger V)^{ib}G_Z(x_i), \tag{4.12}$$

where s_W corresponds to the Weinberg angle and the functions are defined as

$$G_{\gamma 1}(x) = -\frac{16 - 45x + 36x^2 - 7x^3 + 6(2-3x)\log x}{36(1-x)^4}, \tag{4.13}$$

$$G_{\gamma 2}(x) = -\frac{2 - 9x + 18x^2 - 11x^3 + 6x^3\log x}{36(1-x)^4}, \tag{4.14}$$

$$G_Z(x) = \frac{x(1 - x + \log x)}{2(1-x)^2}. \tag{4.15}$$

We note that the SM predictions are flavor universal and the size of the each coefficient at the bottom mass scale is estimated as $(C_9)_{\rm SM} \approx 4$ and $(C_{10})_{\rm SM} \approx -4$, respectively.

The excesses in both P_5' and $R(K^{(*)})$ require destructive interferences with the SM predictions; for instance, the 1σ region of $|\Delta C_9^\mu|$ suggested by the global analysis is $-0.81 \le \Delta C_9^\mu \le -0.48$ (1σ) and $-1.00 \le \Delta C_9^\mu \le -0.32$ (2σ), assuming $\Delta C_9^\mu = -\Delta C_{10}^\mu$ [74]. There are a lot of works on the global fitting [69–77]. The results are consistent

JHEP05(2018)173

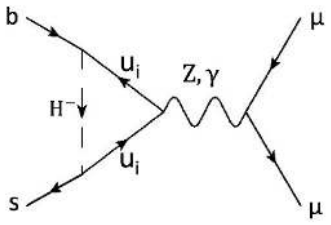

Figure 4. Diagram that contributes to the $B \to K\mu\mu$ in all cases.

with each other and the excesses require large contributions to the muon couplings: $(\Delta C_9^l)/(C_9)_{\rm SM} \simeq -0.2$ and $(\Delta C_{10}^l)/(C_{10})_{\rm SM} \simeq 0.2$. We note that ΔC_{10}^l need not be large, while such a large ΔC_9^l is favored. In fact, the scenario with vanishing ΔC_{10}^l can fit the experimental results at the 2σ level [75].

It is important that these observables have different characteristics: $R(K^{(*)})$ requires the violation of the flavor universality, but P_5' does not need the violation. In our study, we concentrate on the three cases:

(A) $\rho_e^{ij} = 0$ and $\rho_\nu^{ij} = 0$,

(B) $\rho_e^{\mu\tau} \neq 0$, $\rho_e^{\tau\mu} \neq 0$ and $\rho_\nu^{ij} = 0$,

(C) $\rho_e^{ij} = 0$ and $(\widetilde{\rho}_\nu)^{\mu j} \neq 0$.

In the case (A), the extra scalars do not couple to leptons, so that we can not expect the violation of the lepton universality. P_5' in this framework has been studied in refs. [37, 38], and we find the sizable ρ_u^{tc}, ρ_u^{ct} and ρ_u^{tt} lead large ΔC_9 and ΔC_{10}.

In the case (B), $\rho_e^{\mu\tau}$ and $\rho_e^{\tau\mu}$ are only non-vanishing. In such a case, we can expect that the discrepancy of $(g-2)_\mu$ is explained by the one-loop correction involving the neutral scalars [49, 50]. Besides, the violation of the lepton universality in $B \to K^{(*)}ll$ would be realized, if ρ_u^{tc}, ρ_u^{ct} and ρ_u^{tt} are sizable.

In the case (C), we assume that $(\widetilde{\rho}_\nu)^{\mu j}$ is only sizable. In this case, the box diagram involving the charged Higgs leads the destructive interference with the SM prediction in C_9^μ and C_{10}^μ, so that the anomaly of $R(K^{(*)})$ may be resolved.

Below, we discuss the induced C_9, C_{10} and the relevant constraints in the each case. We do not consider the case that both $(\widetilde{\rho}_\nu)^{\mu j}$ and $\rho_e^{\mu\tau,\tau\mu}$ are sizable, in order to avoid the left-right mixing couplings of leptons induced by the one-loop diagrams involving the extra scalars.

4.3.1 Case (A): $\rho_e^{ij} = 0$ and $\rho_\nu^{ij} = 0$

In the case (A), the violation of the lepton universality can not be expected, but large ΔC_9 and ΔC_{10} may be induced by the loop diagrams involving the scalars. In our setup, the main contributions to the operators are given by the couplings, ρ_u^{tc}, ρ_u^{ct}, and ρ_u^{tt}. Then, the charged Higgs plays a crucial role in ΔC_9 and ΔC_{10}. The dominant contribution is given by the penguin diagram in figure 4. We note that this type diagram is allowed in all cases.

JHEP05(2018)173

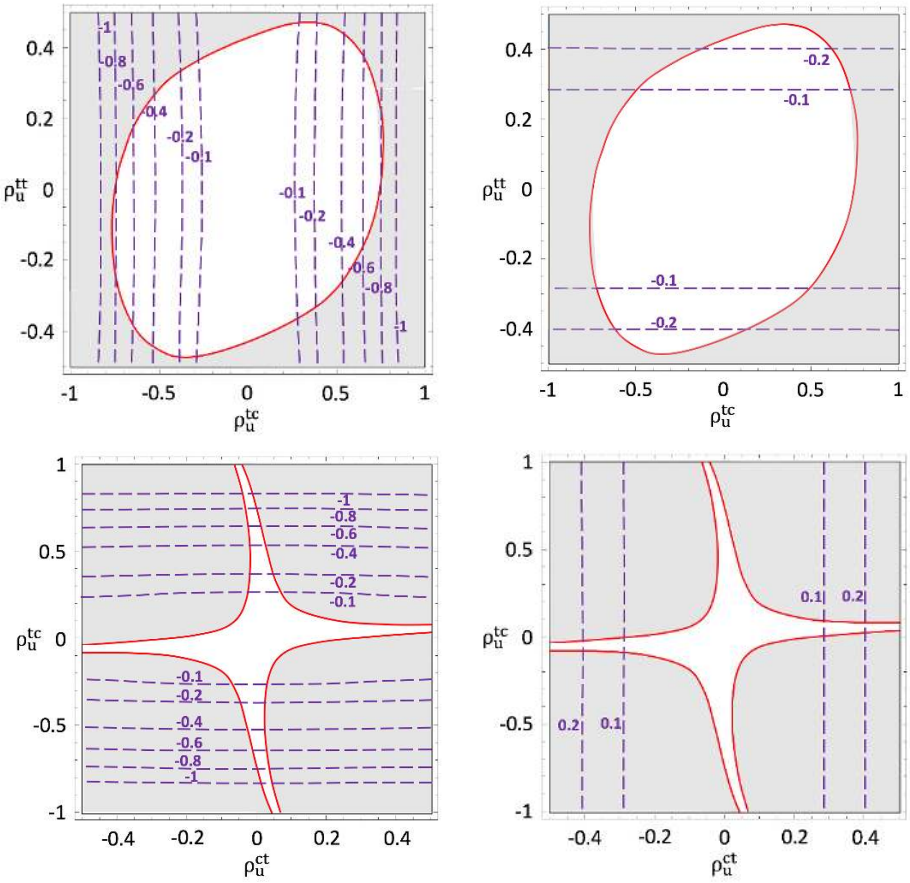

Figure 5. ρ_u^{tt} vs. ρ_u^{ct} (upper) and ρ_u^{tc} vs. ρ_u^{ct} (lower) in the case (A) with $m_{H^\pm} = 200\,\text{GeV}$. The gray region is excluded by the $B_s - \overline{B_s}$ mixing and the red lines correspond to the borders. The dashed purple lines denote the predictions of ΔC_9 (left) and ΔC_{10} (right).

Setting the charged Higgs mass at $m_{H^\pm} = 200\,\text{GeV}$, we draw the predicted ΔC_9 and ΔC_{10} in figure 5. The relevant constraints are shown in those plots. The gray region is excluded by the $B_s - \overline{B_s}$ mixing in figure 5. Note that the constraint from the $b \to s\gamma$ process is out of the figures. The dashed purple lines denote the predictions of ΔC_9 and ΔC_{10} on the left and right panels. The size of the deviation is denoted on the each line. In the figures on the upper (lower) line, ρ_u^{ct} (ρ_u^{tt}) is assumed to be vanishing. We see that ρ_u^{tt} does not help the enhancement of ΔC_9, but either ρ_u^{tc} or ρ_u^{ct} can achieve $\Delta C_9 \approx -1$, that can explain the P_5' excess within 1σ level. We note that ρ_u^{tc} is not sensitive to ΔC_{10}.

Let us comment on the contribution to the $B_s \to \mu\mu$ process. The positive (negative) ΔC_{10}^μ coefficient suppresses (enhances) the branching ratio, compared to the SM prediction. The experimental result still has a large uncertainty, and the central value is below the SM prediction [78]. Thus, the positive ΔC_{10}^μ is, in effect, favored, taking into account the $B_s \to \mu\mu$ process as well [75]. If we chose the parameter to predict $\Delta C_{10}^\mu \simeq 0.1$, the suppression is about 2.4%.

JHEP05(2018)173

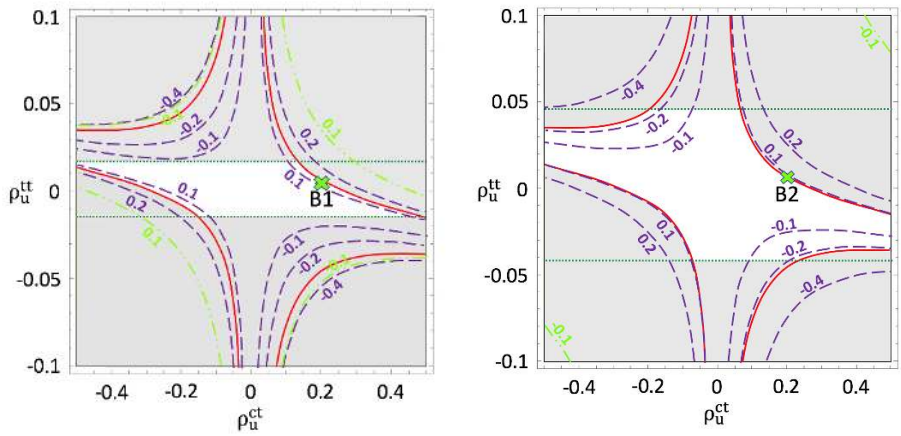

Figure 6. ρ_u^{tt} vs. ρ_u^{ct} in the case (B) with $\rho_e^{\tau\mu} = 1$(left), 0.1(right) and $(m_A, m_H, m_{H_\pm}) = (200\,\text{GeV}, 250\,\text{GeV}, 200\,\text{GeV})$. $\rho_e^{\mu\tau}$ is fixed at $\rho_e^{\mu\tau} = -0.034, -0.34$ that correspond to $\delta\alpha_\mu = (2.61) \times 10^{-9}$. The gray region is excluded by the $B_s - \overline{B_s}$ mixing (red lines) and $\tau \to \mu\gamma$ process (dotted green lines). The dashed green lines and dashed purple lines denote the predictions of ΔC_9 and ΔC_{10} for the each case. The size of the deviation is shown on the each line.

4.3.2 Case (B): $\rho_e^{\mu\tau} \neq 0$, $\rho_e^{\tau\mu} \neq 0$ and $\rho_\nu^{ij} = 0$

In the case (B), we consider the scenario that both $\rho_e^{\mu\tau}$ and $\rho_e^{\tau\mu}$ are sizable, motivated by the $(g-2)_\mu$ anomaly. Note that the mass difference between H and A is also required to explain the excess [49, 50]. As discussed in section 4.1 and section 4.2, ρ_u^{tc} leads the conflict with $B \to D^{(*)}l\nu$ processes, if $\rho_e^{\mu\tau,\tau\mu}$ are sizable. The deviation of $(g-2)_\mu$, denoted by $\delta\alpha_\mu$, is evaluated at the one-loop level as

$$\delta\alpha_\mu = 2.61\left(\frac{\rho_e^{\tau\mu}\rho_e^{\mu\tau}}{-0.034}\right)\times 10^{-9}, \tag{4.16}$$

when (m_A, m_H) is fixed at $(m_A, m_H) = (200\,\text{GeV}, 250\,\text{GeV})$. The value experimentally required [79][3] is $\delta\alpha_\mu = (2.61 \pm 0.8) \times 10^{-9}$, so that $\rho_e^{\tau\mu}\rho_e^{\mu\tau}$ should be about 0.03 to explain the discrepancy at the 1σ level.

In figure 6, we investigate the sizes of ΔC_9^μ and ΔC_{10}^μ, setting $\rho_e^{\tau\mu} = 1$, 0.1 and $(m_A, m_H, m_{H^\pm}) = (200\,\text{GeV}, 250\,\text{GeV}, 200\,\text{GeV})$. $\rho_e^{\mu\tau}$ is fixed at $\rho_e^{\mu\tau} = -0.034, -0.34$ that correspond to $\delta\alpha_\mu = 2.61 \times 10^{-9}$. In the plots, the ρ_u^{tt} and ρ_u^{ct} dependences are shown, to see the contribution of the box diagram in figure 7. ρ_u^{tc} is vanishing on the both panels. The gray region is excluded by the B_s-$\overline{B_s}$ mixing (red lines) and $\tau \to \mu\gamma$ process (dotted green lines). The dashed green lines and dashed purple lines denote the predictions of ΔC_9^μ and ΔC_{10}^μ for the each case.

In this case, the deviations of ΔC_9^μ and ΔC_{10}^μ can be sizable, according to the diagrams in figure 4 and figure 7. In particular, the box diagram in figure 7 can lead the flavor universality violation in the $B \to K^{(*)}ll$ processes. In the case (B), however, the box diagram in figure 7 predicts two muons in the final state to be right-handed, so that

[3] See also refs. [80–82] for a recent development.

JHEP05(2018)173

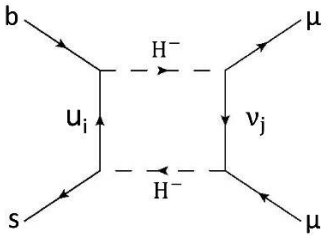

Figure 7. Diagram that contributes to the $B \to K\mu\mu$ in case (B) and case (C).

the relation, $\Delta C_9^\mu = \Delta C_{10}^\mu$, is predicted. According to the recent global analyses [74, 75], $\Delta C_9^\mu = -\Delta C_{10}^\mu$ is favored. $R(K)$ is, in fact, estimated as $R(K) = 1 + 0.23\Delta C_9^\mu - 0.233\Delta C_{10}^\mu$ in $1\,\mathrm{GeV}^2 \leq q^2 \leq 6\,\mathrm{GeV}^2$ [83], so that the relation, $\Delta C_9^\mu = \Delta C_{10}^\mu$, leads $R(K)$ to almost unit. Thus, we conclude that it is difficult to achieve the explanations of the $R(K^{(*)})$ anomaly in the case (B). Such a positive ΔC_{10} is disfavored by $B_s \to \mu\mu$. As mentioned above, it is also difficult that the explanation of $R(D)$ is compatible with the one of $(g-2)_\mu$, because of the constraint from the lepton universality of $B \to D^{(*)}l\nu$. Note that ΔC_9^μ is small on this plane in figure 6. If ρ_u^{tc} is not vanishing, sizable ΔC_9^μ can be derived as shown in figure 5, although the ΔC_9^μ is flavor universal. Then, it is possible that we explain both the $R(D)$ and P_5' anomalies by the one parameter set, but $R(K^{(*)})$ is not compatible with the explanation.

4.3.3 Case (C): $\rho_e^{ij} = 0$ and $(\widetilde{\rho_\nu})^{j\mu} \neq 0$

Finally, we study the case (C). The all elements of ρ_e are vanishing and some elements of ρ_ν are sizable in this case. As discussed in section 3.2, the LFV processes strictly constrain $(\widetilde{\rho_\nu})^{ij}$, and then we assume that the only sizable element is $(\widetilde{\rho_\nu})^{\mu j}$. This assumption principally forbids the flavor violating processes. $(\widetilde{\rho_\nu})^{\mu j}$ is also constrained by the (semi)leptonic B decays, as shown in section 4.1 and section 4.2, when ρ_u^{tc} is large. Let us define the following parameter,

$$\overline{\rho_\nu} = \sqrt{\sum_j |(\widetilde{\rho_\nu})^{\mu j}|^2}, \tag{4.17}$$

and draw figure 8 fixing $\overline{\rho_\nu} = 1$, 2 on the left and right panels, respectively.

Based on ref. [83], we evaluate $R(K)$, that is the ratio between $\mathrm{BR}(B^+ \to K^+\mu\mu)$ and $\mathrm{BR}(B^+ \to K^+ ee)$. $R(K)$ is reported in each bin of $q^2\,\mathrm{GeV}^2$, which is the invariant mass of two leptons in the final state [48]. In particular, the result in $B^+ \to K^+\mu\mu$ with $1\,\mathrm{GeV}^2 \leq q^2 \leq 6\,\mathrm{GeV}^2$ is smaller than the SM predictions: $R(K) = 0.745^{+0.090}_{-0.074} \pm 0.036$ [48]. The lepton universality is measured in $B_0 \to K^*\mu\mu$ as well, and the experimental result also shows the similar sign about the lepton universality violation [47].

In our model, $R(K)$ is deviated by the diagram in figure 7 via the leptonic Yukawa couplings. In the case (C), the leptons in the final state can be left-handed, so that $\Delta C_9 = -\Delta C_{10}$ is predicted. In figure 8, the predicted $R(K)$ is drawn by the dashed purple lines. The number on the each line corresponds to the size of $R(K)$. The relevant parameters are fixed at $\overline{\rho_\nu} = 1$(left panel), 2(right panel) and $(m_A, m_H, m_{H^\pm}) =$

JHEP05(2018)173

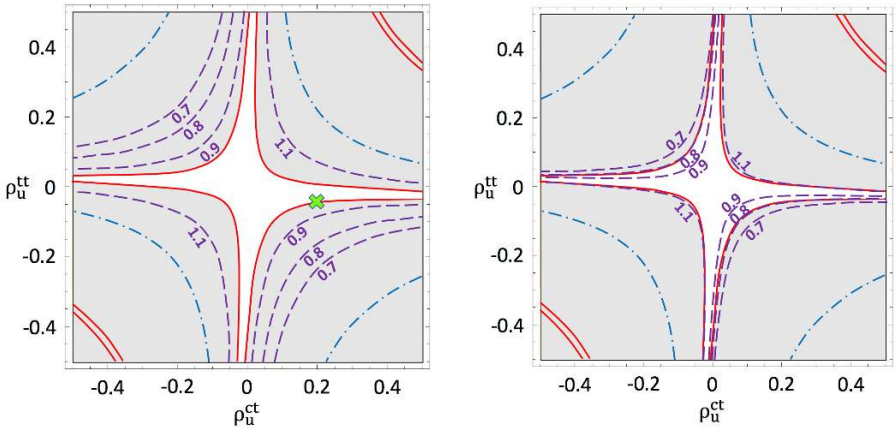

Figure 8. ρ_u^{tt} vs. ρ_u^{ct} in the case (C) with $\overline{\rho_\nu} = 1$(left), 2(right) and $(m_A, m_H, m_{H^\pm}) = (200\,\text{GeV}, 200\,\text{GeV}, 200\,\text{GeV})$. The gray region is excluded by the $B_s - \overline{B_s}$ mixing (solid red lines) and $b \to s\gamma$ (dotted-dashed blue lines). The dashed purple lines denote the predictions of $R(K)$.

(200 GeV, 200 GeV, 200 GeV). The gray region is excluded by the $B_s - \overline{B_s}$ mixing (solid red lines) and $b \to s\gamma$ (dotted-dashed blue lines). As we see in figure 8, large $\overline{\rho_\nu}$ is required even in the light charged Higgs scenario. The strongest constraint comes from B_s-$\overline{B_s}$ mixing, and then $R(K)$ can reach 0.8, that is within 1σ region, when $\overline{\rho_\nu} = 2$ and $m_{H^\pm} = 200\,\text{GeV}$.

In such a case with large $\overline{\rho_\nu}$, the cosmological observations and the neutrino experiments will severely constrain our model. Let us simply assume that the active neutrinos consist of right-handed and left-handed neutrinos: they are Dirac neutrinos. In the case (C), the coupling with muon, $\widetilde{\rho_\nu}^{\mu i}$, is large and the others are small. This means that the only one right-handed neutrino that couples to muon is introduced effectively. In our scenario, the right-handed neutrino interacts with the SM particles through the $\overline{\rho_\nu}$ coupling, and it is in the thermal equilibrium up to a few MeV, when $\widetilde{\rho_\nu}^{\mu i}$ is $\mathcal{O}(1)$. The effective number, N_{eff}, of neutrinos in our universe is measured by the Planck experiment: $N_{\text{eff}} = 3.36 \pm 0.34$ (CMB only) [84]. If the decoupling temperature of the right-handed neutrino is small, N_{eff} could be estimated as $N_{\text{eff}} \approx 4$, that is excluded by the recent cosmological observation. In order to raise the decoupling temperature and decrease N_{eff}, $\widetilde{\rho_\nu}^{\mu i}$ may be required to be less than $\mathcal{O}(0.1)$ [85].

The right-handed neutrino, on the other hand, is not needed to be an active neutrino, in our setup. In figure 8, the right-handed neutrino mass is vanishing, but the result would not be modified so much even if the small Majorana mass of the right-handed neutrino is introduced. Let us define the right-handed neutrino that couples to muon as ν_R^1. Then, the relevant terms are given by

$$\bar{L}_L^i (V_\nu)^{ij} \widetilde{H}_1 y_\nu^j \nu_R^i + m_R \overline{\nu_R^{1c}} \nu_R^1 + \widetilde{\rho}_\nu^{\mu 1} \overline{L_L^\mu} \widetilde{H}_2 \nu_R^1 + h.c.. \tag{4.18}$$

Here, y_ν^1 can be assumed to be vanishing without conflict with the neutrino observables. As far as H_2 does not develop non-vanishing VEV, $\widetilde{\rho}_\nu^{\mu 1}$ does not contribute to the masses of the active neutrinos, even if m_R is sizable. The decay of ν_R^1 may be suppressed according to

JHEP05(2018)173

the alignment of ρ_ν. It would be interesting to discuss the compatibility between the dark matter abundance and R_K, as discussed in ref. [86]. In our case, ν_R^1 can decay to leptons through ρ_ν^{ij},[4] as far as ν_R^1 is heavier than ν_R^2 and ν_R^3, that decouple with the thermal bath above the QCD phase transition temperature.[5]

The neutrino scattering with nuclei also strongly constrains our model. The relevant process is the neutrino trident production: $\nu N \to \nu\mu\overline{\mu}$ [89]. In our model with sizable $\widetilde{\rho}_\nu^{\mu 1}$, the charged Higgs exchanging enlarges the cross section but the contribution does not interfere with the SM correction, so that the prediction is not deviated from the SM prediction so much. $\widetilde{\rho}_\nu^{\mu 1}$, however, is very large to violate the lepton universality of $B \to K^{(*)}ll$, so that we obtain the limit on the deviation of R_K and R_{K^*}. When $m_{H^\pm}$ is set to 200 GeV, the upper bound on $\widetilde{\rho}_\nu^{\mu 1}$ is about 1 to avoid the 2σ deviation of the experimental result [90]. Thus, the $\widetilde{\rho}_\nu^{\mu 1} \approx 2$ scenario is totally excluded, as far as m_R is not introduced.

We conclude that the scenario with large ν_R^1 coupling is excluded by the cosmological observations and the neutrino experiments, if ν_R^1 is a part of the active neutrinos. We can easily introduce the mass term of ν_R^1, i.e. m_R, since ν_R^1 is neutral under the SM gauge symmetry. Then, the bound from the trident production can be evaded, since ν_R^1 is not an active neutrino in this case. When small other elements of $(\widetilde{\rho}_\nu)^{i2}$ and $(\widetilde{\rho}_\nu)^{i3}$ are allowed and ν_R^1 is heavier than $\nu_R^{2,3}$, ν_R^1 can decay to the SM leptons in association with $\nu_R^{2,3}$. $\nu_R^{2,3}$ can be interpreted as the active neutrinos, if the Majorana masses of $\nu_R^{2,3}$ are vanishing. Then, $(\widetilde{\rho}_\nu)^{ij}$, except for $(\widetilde{\rho}_\nu)^{\mu 1}$, should be smaller than $\mathcal{O}(0.1)$.

If the decay of ν_R^1 is much suppressed, the abundance of ν_R^1 would be constrained by the cosmology. The cold dark matter case is similar to the result in ref. [86]. In this paper, the consistency with the cosmological observation in such a dark matter case is beyond our scope. In section 5, we propose the direct search for ν_R^1 at the LHC.

4.4 Summary of the capabilities to explain the excesses

We summarize the possibility that our model can explain the excesses in the flavor physics, choosing the proper parameter set. In table 5, our conclusion about the each excess is shown. On the first, second and third rows, ρ_u^{tt}, ρ_u^{tc} and ρ_u^{ct} are only sizable in the case (B) and (C), respectively. The each column corresponds to the capability to explain the each excess denoted on the top row. The symbol, "◯", means that our predictions are within the 1σ regions of the experimental results. In the box with "×", our prediction is out of the 2σ region. In the box with "△", the predictions can be within the 2σ region of the experimental results, i.e., P_5' and $R(K) = 0.745^{+0.090}_{-0.074} \pm 0.036 \simeq 0.745^{+0.097}_{-0.082}(q^2\ [1, 6]\text{GeV}^2)$ [48], if $\overline{\rho_\nu}$ is $\mathcal{O}(1)$. The Dirac neutrino case predicts $N_{\text{eff}} \approx 4$ and is in tension with the recent cosmological observation. The neutrino trident production also excludes the case with $\overline{\rho_\nu} > 1$. We can also introduce the small Majorana mass term, m_R, to decrease N_{eff}.

In the end, it is difficult to explain all of the excesses in our parameterization. The explanations of P_5' and $R(D)$ can be done by the sizable ρ_u^{tc} and the $\rho_e^{\mu\tau}$, but cannot be

[4] $\widetilde{\rho}_\nu^{i2}$ and $\widetilde{\rho}_\nu^{i3}$ are negligibly small, but not vanishing.

[5] Recently, the model with light ν_R that strongly couples to leptons is discussed, motivated by the $R(D^{(*)})$ anomaly [87, 88].

JHEP05(2018)173

	$R(K^{(*)})$	P_5'	$R(D)$	$R(D^*)$	$\delta\alpha_\mu$
(B) $\rho_e \neq 0$, $\rho_\nu = 0$					
ρ_u^{tt}	$\times$	$\times$	$\times$	$\times$	◯
ρ_u^{tc}	$\times$	◯	◯	$\times$	$\times$
ρ_u^{ct}	$\times$	$\times$	$\times$	$\times$	◯
(C) $\rho_e = 0$, $\rho_\nu \neq 0$					
ρ_u^{tt}	△	△	$\times$	$\times$	$\times$
ρ_u^{tc}	$\times$	◯	◯	$\times$	$\times$
ρ_u^{ct}	△	△	$\times$	$\times$	$\times$

Table 5. Summary of the capabilities to explain the excesses. In the each observable, our prediction is evaluated by the symbols, "◯", "△" and "×". The meanings are explained in the text.

compatible with the solutions to the $(g-2)_\mu$ and $R(K^{(*)})$ anomalies. This is because the charged Higgs that couple to b, c and μ largely violate the lepton universality of $B \to D^{(*)} l\nu$.

5 Our signals at the LHC

Before closing our paper, we discuss the possibility that our 2HDM is tested by the LHC experiments. In our scenarios, the extra scalars are relatively light: we fix the masses at 200 GeV or 250 GeV. Thus, the main targets to prove our model are the direct signals originated from the scalars.

In the case (A), there are Yukawa couplings between the scalars and heavy quarks, denoted by ρ_u^{tc}, ρ_u^{ct} and ρ_u^{tt}. If either ρ_u^{tc} or ρ_u^{ct} is $\mathcal{O}(1)$, we obtain large ΔC_9, that can explain the P_5' excess. In this case, the neutral and charged scalars are produced in association with top quark or bottom quark in the final state. The produced scalars dominantly decay to heavy quarks, so that there are tt/bb/tb quarks in the final state. Such a case has been studied in ref. [37].[6]

In the case (B), the neutral scalars can decay to μ and τ, and the charged Higgs decays to μ or τ with one neutrino. The scalars are produced via ρ_u^{ct} coupling, and then the production cross sections of the scalars at the LHC with $\sqrt{s} = 13\,\text{TeV}$ (8 TeV) are estimated in table 6, using CALCHEP [104]. Note that cteq6l1 is applied to the parton distribution function. Here, we quantitatively study our signal on the benchmark points in figure 6.We put the green x-marks on the figures. On the benchmark point (B1), the parameters are aligned as

$$\begin{aligned} m_{H^\pm} = m_A = 200\,\text{GeV},\ m_H = 250\,\text{GeV}, \\ (\rho_u^{tt},\, \rho_u^{ct}) = (0.005,\, 0.2), \\ (\rho_e^{\tau\mu},\, \rho_e^{\mu\tau}) = (1,\, -0.0341). \end{aligned} \tag{5.1}$$

[6] See also refs. [91–103].

JHEP05(2018)173

$\sqrt{s}$	13TeV	8TeV
$m_{H^\pm} = 200$ [GeV]		
$\sigma(b+\bar{c} \to H^\pm)$	$792\times\lvert\rho_u^{tc}\rvert^2$	$287\times\lvert\rho_u^{tc}\rvert^2$
$\sigma(g+s \to t+H^-)$	$11.4\times\lvert\rho_u^{ct}\rvert^2$	$3.0\times\lvert\rho_u^{ct}\rvert^2$
$\sigma(g+g \to \bar{s}+t+H^-)$	$4.0\times\lvert\rho_u^{ct}\rvert^2$	$0.88\times\lvert\rho_u^{ct}\rvert^2$
$m_\phi = 200$ [GeV] ($\phi = H,\, A$)		
$\sigma(g+c \to t+\phi)$	$3.8\times\lvert\rho_u^{ct}\rvert^2$	$0.92\times\lvert\rho_u^{ct}\rvert^2$
$\sigma(g+g \to \bar{c}+t+\phi)$	$1.36\times\lvert\rho_u^{ct}\rvert^2$	$0.3\times\lvert\rho_u^{ct}\rvert^2$
$m_\phi = 250$ [GeV]		
$\sigma(g+c \to t+\phi)$	$0.84\times\lvert\rho_u^{ct}\rvert^2$	$0.17\times\lvert\rho_u^{ct}\rvert^2$
$\sigma(g+g \to \bar{c}+t+\phi)$	$2.4\times\lvert\rho_u^{ct}\rvert^2$	$0.55\times\lvert\rho_u^{ct}\rvert^2$

Table 6. Heavy Higgs Production cross section in pb. We added normal and conjugate cross sections, just as adding $\sigma(g+s \to t+H^-)$ and $\sigma(g+\bar{s} \to \bar{t}+H^+)$ and denote as $\sigma(g+s \to t+H^-)$.

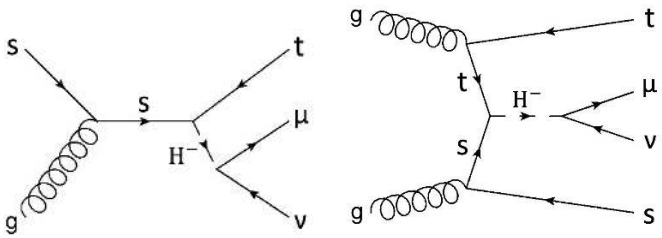

Figure 9. Diagrams that contributes to the $\mu\nu$ resonance.

This parameter set leads a sizable deviation of $(g-2)_\mu$: $\delta\alpha_\mu = 2.61\times10^{-9}$. On this point, the charged Higgs mainly decays to $\mu\nu$ through the diagram in figure 9 and the heavy neutral scalar decays to $\mu\tau$:

$$\begin{aligned} BR(H^- \to \mu\bar{\nu}) \approx 99.3\%, \quad BR(H^- \to \bar{t}s) \approx 1\%, \\ BR(A \to \mu\tau) \approx 99.3\%, \quad BR(A \to tc) \approx 0.7\%, \\ BR(H \to \mu\tau) \approx 96.9\%, \quad BR(H \to tc) \approx 3.1\%. \end{aligned} \tag{5.2}$$

Following table 6, the production cross section of the charged Higgs is estimated as 2.46 pb at the LHC with $\sqrt{s} = 13\,\text{TeV}$. The search for a new heavy resonance decaying to e/μ and neutrino has been developed recently [105] and the upper bound on the production is about 0.6 pb, that naively leads the upper bound on $|\rho_u^{ct}|$ as $|\rho_u^{ct}| \lesssim 0.2$. In our model, however, there are top quarks in the final state, so that the top quark will make the signals fuzzy. The search for a new resonance decaying to $\tau\,\nu/\ \tau\,\mu$ is also attractive, because the decay is predicted by the charged Higgs and the neutral Higgs. It is challenging and actually the heavy mass region is surveyed by the ATLAS [106] and CMS collaborations [107, 108]. As discussed in section 4.2, the excesses in $B \to D^{(*)}\tau\nu$ require rather large Yukawa couplings,

JHEP05(2018)173

so that we expect that the direct search for the resonance at the LHC can reach the favored parameter region near future. The detail analysis is work in progress.

On the benchmark point (B2), the parameters are fixed at

$$\begin{aligned} m_{H^\pm} = m_A = 200\,\text{GeV},\ m_H = 250\,\text{GeV}, \\ (\rho_u^{tt},\, \rho_u^{ct}) = (0.006,\, 0.2), \\ (\rho_e^{\tau\mu},\, \rho_e^{\mu\tau}) = (0.1,\, -0.341). \end{aligned} \tag{5.3}$$

Then, the sizable deviation of $(g-2)_\mu$ is estimated as $\delta\alpha_\mu = 2.61 \times 10^{-9}$. Since $\rho_e^{\mu\tau}$ is sizable, the charged Higgs decays to $\tau\nu$:

$$\begin{aligned} &BR(H^- \to \mu\bar{\nu}) \approx 7.5\%, \quad BR(H^- \to \tau\bar{\nu}) \approx 86.9\%, \quad BR(H^- \to \bar{t}s) \approx 5.6\%, \\ &BR(A \to \mu\tau) \approx 94.4\%, \quad BR(A \to tc) \approx 5.6\%, \\ &BR(H \to \mu\tau) \approx 79.6\%, \quad BR(H \to tc) \approx 20.4\%. \end{aligned} \tag{5.4}$$

In this case, the charged Higgs mainly decays to $\tau\nu$, and can evade the bound from the $\mu\nu$ resonance search.

In the case (C), the scalars are produced due to the large ρ_u^{ct}. The produced neutral scalars decay to two neutrinos in this case, so that they predict the invisible signal. The charged scalar decays to one muon and one neutrino. This signal is similar to the case (B). On the benchmark point in figure 8, the parameters satisfy

$$\begin{aligned} m_{H^\pm} = m_A = m_H = 200\,\text{GeV}, \\ (\rho_u^{tt},\, \rho_u^{ct}) = (-0.04,\, 0.2), \\ \overline{\rho_\nu}^2 = 1. \end{aligned} \tag{5.5}$$

These parameters lead the following branching ratios,

$$\begin{aligned} &BR(H^- \to \mu\bar{\nu}) \approx 99\%, \quad BR(H^- \to \bar{t}s) \approx 1\%, \\ &BR(\phi_h \to \nu\nu) \approx 99\%, \quad BR(\phi_h \to tc) \approx 1\%\ (\phi_h = H,\, A). \end{aligned} \tag{5.6}$$

The invisible decay of the heavy neutral scalars, produced by the diagram in figure 10, leads the mono-top signal: $pp \to \phi_h t \to \nu\bar{\nu}t$. The current upper bound on the cross section at the LHC with $\sqrt{s} = 8\,\text{TeV}$ is $\sigma(pp \to t + \text{missing}) \leq 0.8$ [pb] [109, 110] when $m_H = 200\,\text{GeV}$. Based on the results in table 6, the mono-top signal on this benchmark point is about 0.3 pb, so that it is just below the current upper bound.

In our model, the same-sign top signal is also predicted by the diagrams in figure 11, depending on the mass spectrum of the scalars. If the neutral scalars, H and A, are not degenerate, the same-sign top signal, $pp \to tt$, is enhanced by ρ_u^{ct}, ρ_u^{tc} couplings. The current upper bound on the cross section is 1.2 pb at the LHC with $\sqrt{s} = 13\,\text{TeV}$ [111]. When $m_A = 200\,\text{GeV}$ and $m_H = 250\,\text{GeV}$, the each cross section is estimated as

$$\begin{aligned} \sigma(pp \to tt + \overline{tt}) &= 4.23 \times 10^{-3} |\rho_u^{tc}|^4 [\text{pb}], \\ \sigma(pp \to tt\bar{c} + \overline{tt}c) &= 4.13 \times 10^{-1} |\rho_u^{tc}|^4 [\text{pb}], \\ \sigma(pp \to tt\bar{c}\bar{c} + \overline{tt}cc) &= 1.14 \times 10^{-1} |\rho_u^{tc}|^4 [\text{pb}]. \end{aligned} \tag{5.7}$$

JHEP05(2018)173

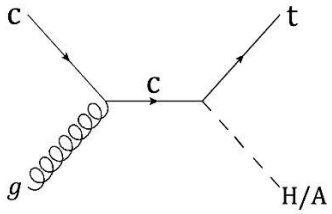

Figure 10. Diagram that contributes to our monotop.

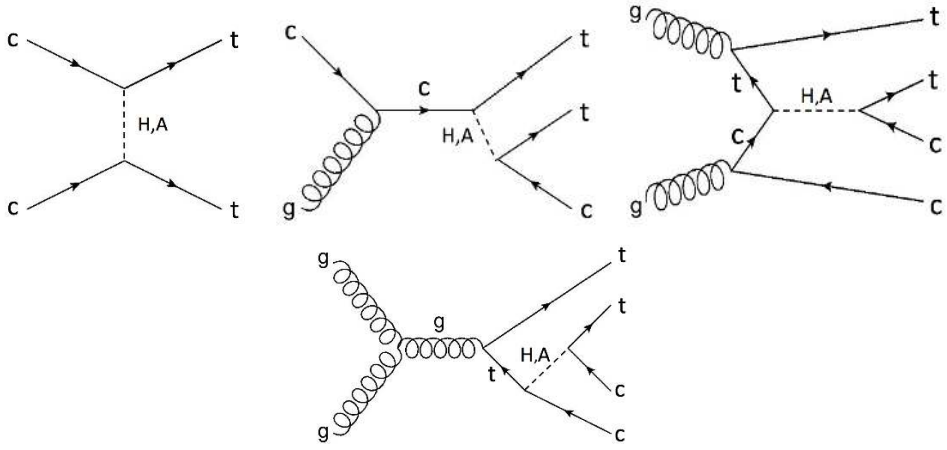

Figure 11. Feynman diagrams relevant to the same-sign top signal.

Then, our predictions on the benchmark points are below the experimental bound. We note that the same-sign top signal is produced by the process, $pp \to tt\bar{c} + \bar{t}\bar{t}c$, rather than $pp \to cc \to tt + \bar{t}\bar{t}$, because of the production processes as shown in figure 11.

6 Summary

We have studied the flavor physics in type-III 2HDM. In this model, there are many possible parameter choices, so we adopt some simple parameter sets motivated by the physical observables where the deviations from the SM predictions are reported. In our scenario, the flavor violating Yukawa couplings for up-type quarks, ρ_u^{tc} and ρ_u^{ct}, play an important role in enhancing/suppressing the semileptonic B decays, e.g. $B \to K^* ll$. In particular, ρ_u^{ct} can evade the strong bound from the flavor physics and the collider experiments, so that ρ_u^{ct} is expected to be larger than $\mathcal{O}(0.1)$. In addition, we introduce the flavor violating Yukawa couplings to the lepton sector as well: $\rho_e^{\tau\mu}$ and $\rho_e^{\mu\tau}$. As discussed in refs. [49, 50], those flavor violating couplings deviate $(g-2)_\mu$, as far as the extra neutral scalars are not degenerate. In our paper, we have discussed the compatibility between the explanations of $(g-2)_\mu$, of the $B \to K^{(*)} ll$ and of the $B \to D^{(*)} \tau\nu$ excesses. As shown in table 5, the explanations of $(g-2)_\mu$ and $R(D)$ require relatively large Yukawa couplings, so the constraint from the lepton universality of $B \to D^{(*)} l\nu$ easily excludes our model.

JHEP05(2018)173

In order to explain the $R(K)$ excess, we need the sizable lepton flavor universality violation in the $B \to K^{(*)}ll$ processes. Then, we introduce the flavor violating Yukawa couplings involving right-handed neutrino, and discuss the capability to explain the $R(K)$ excess in our model. In this case, we can evade the strong experimental bounds, as far as the appropriate alignment of the Yukawa couplings is chosen. Thus, the explanation of the $R(K)$ deviation is achieved by the box diagram involving the right-handed neutrinos via the flavor violating neutrino Yukawa couplings. This scenario, however, can not be compatible with the other explanations, because of the stringent constraint from the lepton universality of $B \to D^{(*)}l\nu$. In addition, the Dirac neutrino case is excluded by the recent cosmological observation. Then, the sizable Majorana mass term for the right-handed neutrino is required to decrease the effective neutrino number. The possible parameter choices and the capabilities of the each setup are summarized in table 5.

Finally, we have investigated the possibility that the LHC experiments directly test our model. Interestingly, the direct search for new physics at the LHC can reach the parameter region that is favored by the excesses in the flavor physics [37, 91–97, 100–103]. In our scenario, the scalar are enough light to be produced by the proton-proton collider. In the case that the charged Higgs mainly decays to one muon and one neutrino, the heavy resonance search at the LHC could widely cover our parameter region. The neutral scalar decays to two neutrinos, if the neutrino Yukawa couplings are large. In this case, the mono-top signal could be our promising one, although the current bound has not yet reached our parameter region. The sizable ρ_u^{ct} predicts the same-sign top signal, if the neutral scalars are not degenerate. We have confirmed that our prediction of the cross section is below the current upper bound, but we can expect that our region could be covered near future.

Acknowledgments

The work of Y.O. is supported by Grant-in-Aid for Scientific research from the Ministry of Education, Science, Sports, and Culture (MEXT), Japan, No. 17H05404. The authors thank to Kazuhiro Tobe, Tomomi Kawaguchi, Makoto Tomoto and Yasuyuki Horii for variable discussions.

JHEP05(2018)173

A Various parameters for our numerical analysis

Here, we summarize numerical values of various parameters we use in our numerical calculation below.

Quantity	Value	Refs.	Quantity	Value	Refs.
CKM parameters			parameters for hadronic matrix elements		
λ	0.22506	[63]	ρ_D^2	1.128	[56]
A	0.811	[63]	$\rho_{D^*}^2$	1.205	[56]
$\bar{\rho}$	0.124	[63]	$R_1(1)$	1.404	[56]
$\bar{\eta}$	0.356	[63]	$R_2(1)$	0.854	[56]
B and D meson parameters			Δ	1	[68]
m_{Bd}	5.280 [GeV]	[63]	$h_{A1}(1)$	0.908	[115]
m_{B^-}	5.279 [GeV]	[63]	$V_1(1)$	1.07	[116]
m_{Bs}	5.367 [GeV]	[63]	SM particle masses and $G_{\rm F}$		
M_{Bc}	6.275 [GeV]	[63]	m_μ	0.105676 [GeV]	
m_D	1.865 [GeV]	[63]	m_τ	1.77686 [GeV]	
m_{D^*}	2.007 [GeV]	[63]	$m_c(m_c)$	1.27 [GeV]	
τ_{Bd}	2.309×10^{12} [GeV^{-1}]	[63]	m_t	173.21 [GeV]	
$f_{Bd}\sqrt{B_{Bd}}$	227.7 [MeV]	[112]	m_d(2GeV)	0.0047 [GeV]	
τ_{B^-}	2.489×10^{12} [GeV^{-1}]	[63]	m_s(2GeV)	0.096 [GeV]	[63]
f_{B^-}	186 [MeV]	[113]	$m_b(m_b)$	4.18 [GeV]	
τ_{Bs}	2.294×10^{12} [GeV^{-1}]	[63]	m_W	80.385 [GeV]	
$f_{Bs}\sqrt{B_{Bs}}$	274.6 [MeV]	[112]	m_Z	91.188 [GeV]	
τ_{Bc}	7.703×10^{11} [GeV^{-1}]	[63]	m_h	125.09 [GeV]	
f_{Bc}	0.434 [GeV]	[114]	G_F	1.166×10^{-5} [GeV^{-2}]	

References

[1] ATLAS collaboration, *Observation of a new particle in the search for the Standard Model Higgs boson with the ATLAS detector at the LHC*, *Phys. Lett.* **B 716** (2012) 1 [arXiv:1207.7214] [INSPIRE].

[2] CMS collaboration, *Observation of a new boson at a mass of 125 GeV with the CMS experiment at the LHC*, *Phys. Lett.* **B 716** (2012) 30 [arXiv:1207.7235] [INSPIRE].

[3] T.D. Lee, *A Theory of Spontaneous T Violation*, *Phys. Rev.* **D 8** (1973) 1226 [INSPIRE].

JHEP05(2018)173

[4] H.E. Haber, G.L. Kane and T. Sterling, *The Fermion Mass Scale and Possible Effects of Higgs Bosons on Experimental Observables*, *Nucl. Phys.* **B 161** (1979) 493 [INSPIRE].

[5] J.F. Donoghue and L.F. Li, *Properties of Charged Higgs Bosons*, *Phys. Rev.* **D 19** (1979) 945 [INSPIRE].

[6] L.J. Hall and M.B. Wise, *Flavor Changing Higgs-Boson Couplings*, *Nucl. Phys.* **B 187** (1981) 397 [INSPIRE].

[7] W.-S. Hou, *Tree level $t \to ch$ or $h \to t\bar{c}$ decays*, *Phys. Lett.* **B 296** (1992) 179 [INSPIRE].

[8] D. Chang, W.S. Hou and W.-Y. Keung, *Two loop contributions of flavor changing neutral Higgs bosons to $\mu \to e\gamma$*, *Phys. Rev.* **D 48** (1993) 217 [hep-ph/9302267] [INSPIRE].

[9] D. Atwood, L. Reina and A. Soni, *Probing flavor changing top-charm-scalar interactions in e^+e^- collisions*, *Phys. Rev.* **D 53** (1996) 1199 [hep-ph/9506243] [INSPIRE].

[10] D. Atwood, L. Reina and A. Soni, *Phenomenology of two Higgs doublet models with flavor changing neutral currents*, *Phys. Rev.* **D 55** (1997) 3156 [hep-ph/9609279] [INSPIRE].

[11] S.L. Glashow and S. Weinberg, *Natural Conservation Laws for Neutral Currents*, *Phys. Rev.* **D 15** (1977) 1958 [INSPIRE].

[12] J. Liu and L. Wolfenstein, *Spontaneous CP-violation in the $\mathrm{SU}(2)_L \times \mathrm{U}(1)_Y$ Model with Two Higgs Doublets*, *Nucl. Phys.* **B 289** (1987) 1 [INSPIRE].

[13] T.P. Cheng and M. Sher, *Mass Matrix Ansatz and Flavor Nonconservation in Models with Multiple Higgs Doublets*, *Phys. Rev.* **D 35** (1987) 3484 [INSPIRE].

[14] M.J. Savage, *Constraining flavor changing neutral currents with $B \to \mu^+\mu^-$*, *Phys. Lett.* **B 266** (1991) 135 [INSPIRE].

[15] A. Antaramian, L.J. Hall and A. Rasin, *Flavor changing interactions mediated by scalars at the weak scale*, *Phys. Rev. Lett.* **69** (1992) 1871 [hep-ph/9206205] [INSPIRE].

[16] L.J. Hall and S. Weinberg, *Flavor changing scalar interactions*, *Phys. Rev.* **D 48** (1993) R979 [hep-ph/9303241] [INSPIRE].

[17] M.E. Luke and M.J. Savage, *Flavor changing neutral currents in the Higgs sector and rare top decays*, *Phys. Lett.* **B 307** (1993) 387 [hep-ph/9303249] [INSPIRE].

[18] M. Aoki, S. Kanemura, K. Tsumura and K. Yagyu, *Models of Yukawa interaction in the two Higgs doublet model and their collider phenomenology*, *Phys. Rev.* **D 80** (2009) 015017 [arXiv:0902.4665] [INSPIRE].

[19] N. Haba, H. Umeeda and T. Yamada, *Semialigned two Higgs doublet model*, *Phys. Rev.* **D 97** (2018) 035004 [arXiv:1711.06499] [INSPIRE].

[20] S. Iguro, Y. Muramatsu, Y. Omura and Y. Shigekami, *Flavor physics in the multi-Higgs doublet models induced by the left-right symmetry*, arXiv:1804.07478 [INSPIRE].

[21] BaBar collaboration, J.P. Lees et al., *Evidence for an excess of $\bar{B} \to D^{(*)}\tau^-\bar{\nu}_\tau$ decays*, *Phys. Rev. Lett.* **109** (2012) 101802 [arXiv:1205.5442] [INSPIRE].

[22] BaBar collaboration, J.P. Lees et al., *Measurement of an Excess of $\bar{B} \to D^{(*)}\tau^-\bar{\nu}_\tau$ Decays and Implications for Charged Higgs Bosons*, *Phys. Rev.* **D 88** (2013) 072012 [arXiv:1303.0571] [INSPIRE].

[23] LHCb collaboration, *Measurement of the ratio of branching fractions $\mathcal{B}(\bar{B}^0 \to D^{*+}\tau^-\bar{\nu}_\tau)/\mathcal{B}(\bar{B}^0 \to D^{*+}\mu^-\bar{\nu}_\mu)$*, *Phys. Rev. Lett.* **115** (2015) 111803 [arXiv:1506.08614] [INSPIRE].

JHEP05(2018)173

[24] Belle collaboration, M. Huschle et al., *Measurement of the branching ratio of $\bar{B} \to D^{(*)}\tau^-\bar{\nu}_\tau$ relative to $\bar{B} \to D^{(*)}\ell^-\bar{\nu}_\ell$ decays with hadronic tagging at Belle*, *Phys. Rev.* **D 92** (2015) 072014 [arXiv:1507.03233] [INSPIRE].

[25] Belle collaboration, Y. Sato et al., *Measurement of the branching ratio of $\bar{B}^0 \to D^{*+}\tau^-\bar{\nu}_\tau$ relative to $\bar{B}^0 \to D^{*+}\ell^-\bar{\nu}_\ell$ decays with a semileptonic tagging method*, *Phys. Rev.* **D 94** (2016) 072007 [arXiv:1607.07923] [INSPIRE].

[26] Belle collaboration, S. Hirose et al., *Measurement of the τ lepton polarization and $R(D^*)$ in the decay $\bar{B} \to D^*\tau^-\bar{\nu}_\tau$*, *Phys. Rev. Lett.* **118** (2017) 211801 [arXiv:1612.00529] [INSPIRE].

[27] G. Wormser, *$B \to D^{(*)}\tau\nu$ overview*, talk at *The 15th meeting in the conference series of Flavor Physics & CP Violation (FPCP 2017)*, Prague, Czech Republic, 5–9 June 2017.

[28] S. Jaiswal, S. Nandi and S.K. Patra, *Extraction of $|V_{cb}|$ from $B \to D^{(*)}\ell\nu_\ell$ and the Standard Model predictions of $R(D^{(*)})$*, *JHEP* **12** (2017) 060 [arXiv:1707.09977] [INSPIRE].

[29] A. Crivellin, C. Greub and A. Kokulu, *Explaining $B \to D\tau\nu$, $B \to D^*\tau\nu$ and $B \to \tau\nu$ in a 2HDM of type-III*, *Phys. Rev.* **D 86** (2012) 054014 [arXiv:1206.2634] [INSPIRE].

[30] A. Celis, M. Jung, X.-Q. Li and A. Pich, *Sensitivity to charged scalars in $B \to D^{(*)}\tau\nu_\tau$ and $B \to \tau\nu_\tau$ decays*, *JHEP* **01** (2013) 054 [arXiv:1210.8443] [INSPIRE].

[31] M. Tanaka and R. Watanabe, *New physics in the weak interaction of $\bar{B} \to D^{(*)}\tau\bar{\nu}$*, *Phys. Rev.* **D 87** (2013) 034028 [arXiv:1212.1878] [INSPIRE].

[32] A. Crivellin, A. Kokulu and C. Greub, *Flavor-phenomenology of two-Higgs-doublet models with generic Yukawa structure*, *Phys. Rev.* **D 87** (2013) 094031 [arXiv:1303.5877] [INSPIRE].

[33] A. Crivellin, J. Heeck and P. Stoffer, *A perturbed lepton-specific two-Higgs-doublet model facing experimental hints for physics beyond the Standard Model*, *Phys. Rev. Lett.* **116** (2016) 081801 [arXiv:1507.07567] [INSPIRE].

[34] J.M. Cline, *Scalar doublet models confront τ and b anomalies*, *Phys. Rev.* **D 93** (2016) 075017 [arXiv:1512.02210] [INSPIRE].

[35] P. Ko, Y. Omura, Y. Shigekami and C. Yu, *LHCb anomaly and B physics in flavored Z' models with flavored Higgs doublets*, *Phys. Rev.* **D 95** (2017) 115040 [arXiv:1702.08666] [INSPIRE].

[36] P. Ko, Y. Omura and C. Yu, *$B \to D^{(*)}\tau\nu$ and $B \to \tau\nu$ in chiral $\mathrm{U}(1)'$ models with flavored multi Higgs doublets*, *JHEP* **03** (2013) 151 [arXiv:1212.4607] [INSPIRE].

[37] S. Iguro and K. Tobe, *$R(D^{(*)})$ in a general two Higgs doublet model*, *Nucl. Phys.* **B 925** (2017) 560 [arXiv:1708.06176] [INSPIRE].

[38] Q.-Y. Hu, X.-Q. Li and Y.-D. Yang, *$B^0 \to K^{*0}\mu^+\mu^-$ decay in the Aligned Two-Higgs-Doublet Model*, *Eur. Phys. J.* **C 77** (2017) 190 [arXiv:1612.08867] [INSPIRE].

[39] P. Arnan, D. Bečirević, F. Mescia and O. Sumensari, *Two Higgs doublet models and $b \to s$ exclusive decays*, *Eur. Phys. J.* **C 77** (2017) 796 [arXiv:1703.03426] [INSPIRE].

[40] A. Arhrib et al., *$R_{K^{(*)}}$ anomaly in type-III 2HDM*, arXiv:1710.05898 [INSPIRE].

[41] L. Bian, S.-M. Choi, Y.-J. Kang and H.M. Lee, *A minimal flavored $\mathrm{U}(1)'$ for B-meson anomalies*, *Phys. Rev.* **D 96** (2017) 075038 [arXiv:1707.04811] [INSPIRE].

JHEP05(2018)173

[42] L. Bian, H.M. Lee and C.B. Park, *B-meson anomalies and Higgs physics in flavored* U(1)′ *model*, *Eur. Phys. J.* **C 78** (2018) 306 [arXiv:1711.08930] [INSPIRE].

[43] R. Alonso, B. Grinstein and J. Martin Camalich, *Lifetime of* B_c^- *Constrains Explanations for Anomalies in* $B \to D^{(*)}\tau\nu$, *Phys. Rev. Lett.* **118** (2017) 081802 [arXiv:1611.06676] [INSPIRE].

[44] A.G. Akeroyd and C.-H. Chen, *Constraint on the branching ratio of* $B_c \to \tau\bar{\nu}$ *from LEP1 and consequences for* $R(D^{(*)})$ *anomaly*, *Phys. Rev.* **D 96** (2017) 075011 [arXiv:1708.04072] [INSPIRE].

[45] LHCb collaboration, *Measurement of Form-Factor-Independent Observables in the Decay* $B^0 \to K^{*0}\mu^+\mu^-$, *Phys. Rev. Lett.* **111** (2013) 191801 [arXiv:1308.1707] [INSPIRE].

[46] LHCb collaboration, *Angular analysis of the* $B^0 \to K^{*0}\mu^+\mu^-$ *decay using* $3\,fb^{-1}$ *of integrated luminosity*, *JHEP* **02** (2016) 104 [arXiv:1512.04442] [INSPIRE].

[47] LHCb collaboration, *Test of lepton universality with* $B^0 \to K^{*0}\ell^+\ell^-$ *decays*, *JHEP* **08** (2017) 055 [arXiv:1705.05802] [INSPIRE].

[48] LHCb collaboration, *Test of lepton universality using* $B^+ \to K^+\ell^+\ell^-$ *decays*, *Phys. Rev. Lett.* **113** (2014) 151601 [arXiv:1406.6482] [INSPIRE].

[49] Y. Omura, E. Senaha and K. Tobe, *Lepton-flavor-violating Higgs decay* $h \to \mu\tau$ *and muon anomalous magnetic moment in a general two Higgs doublet model*, *JHEP* **05** (2015) 028 [arXiv:1502.07824] [INSPIRE].

[50] Y. Omura, E. Senaha and K. Tobe, τ- *and* μ*-physics in a general two Higgs doublet model with* $\mu - \tau$ *flavor violation*, *Phys. Rev.* **D 94** (2016) 055019 [arXiv:1511.08880] [INSPIRE].

[51] S. Davidson and H.E. Haber, *Basis-independent methods for the two-Higgs-doublet model*, *Phys. Rev.* **D 72** (2005) 035004 [*Erratum ibid.* **D 72** (2005) 099902] [hep-ph/0504050] [INSPIRE].

[52] P. Ko, Y. Omura and C. Yu, *Top Forward-Backward Asymmetry and the CDF* Wjj *Excess in Leptophobic* U(1)′ *Flavor Models*, *Phys. Rev.* **D 85** (2012) 115010 [arXiv:1108.0350] [INSPIRE].

[53] P. Ko, Y. Omura and C. Yu, *Chiral* U(1) *flavor models and flavored Higgs doublets: The Top FB asymmetry and the* Wjj, *JHEP* **01** (2012) 147 [arXiv:1108.4005] [INSPIRE].

[54] Y. Omura, K. Tobe and K. Tsumura, *Survey of Higgs interpretations of the diboson excesses*, *Phys. Rev.* **D 92** (2015) 055015 [arXiv:1507.05028] [INSPIRE].

[55] C. Bobeth, A.J. Buras, A. Celis and M. Jung, *Patterns of Flavour Violation in Models with Vector-Like Quarks*, *JHEP* **04** (2017) 079 [arXiv:1609.04783] [INSPIRE].

[56] HFLAV collaboration, Y. Amhis et al., *Averages of b-hadron, c-hadron and* τ*-lepton properties as of summer 2016*, *Eur. Phys. J.* **C 77** (2017) 895 [arXiv:1612.07233] [INSPIRE].

[57] B. Altunkaynak, W.-S. Hou, C. Kao, M. Kohda and B. McCoy, *Flavor Changing Heavy Higgs Interactions at the LHC*, *Phys. Lett.* **B 751** (2015) 135 [arXiv:1506.00651] [INSPIRE].

[58] M. Misiak et al., *Updated NNLO QCD predictions for the weak radiative B-meson decays*, *Phys. Rev. Lett.* **114** (2015) 221801 [arXiv:1503.01789] [INSPIRE].

JHEP05(2018)173

[59] T. Blake, G. Lanfranchi and D.M. Straub, *Rare B Decays as Tests of the Standard Model*, *Prog. Part. Nucl. Phys.* **92** (2017) 50 [arXiv:1606.00916] [INSPIRE].

[60] ATLAS collaboration, *Search for flavour-changing neutral current top quark decays $t \to Hq$ in pp collisions at $\sqrt{s} = 8$ TeV with the ATLAS detector*, *JHEP* **12** (2015) 061 [arXiv:1509.06047] [INSPIRE].

[61] CMS collaboration, *Search for top quark decays via Higgs-boson-mediated flavor-changing neutral currents in pp collisions at $\sqrt{s} = 8$ TeV*, *JHEP* **02** (2017) 079 [arXiv:1610.04857] [INSPIRE].

[62] ATLAS collaboration, *Search for top quark decays $t \to qH$, with $H \to \gamma\gamma$, in $\sqrt{s} = 13$ TeV pp collisions using the ATLAS detector*, *JHEP* **10** (2017) 129 [arXiv:1707.01404] [INSPIRE].

[63] PARTICLE DATA GROUP collaboration, C. Patrignani et al., *Review of Particle Physics*, *Chin. Phys.* **C 40** (2016) 100001 [INSPIRE].

[64] CMS collaboration, *Search for Lepton-Flavour-Violating Decays of the Higgs Boson*, *Phys. Lett.* **B 749** (2015) 337 [arXiv:1502.07400] [INSPIRE].

[65] ATLAS collaboration, *Search for lepton-flavour-violating decays of the Higgs and Z bosons with the ATLAS detector*, *Eur. Phys. J.* **C 77** (2017) 70 [arXiv:1604.07730] [INSPIRE].

[66] CMS collaboration, *Search for lepton flavour violating decays of the Higgs boson to $\mu\tau$ and $e\tau$ in proton-proton collisions at $\sqrt{s} = 13$ TeV*, CMS-PAS-HIG-17-001.

[67] BELLE collaboration, A. Abdesselam et al., *Precise determination of the CKM matrix element $|V_{cb}|$ with $\bar{B}^0 \to D^{*+} \ell^- \bar{\nu}_\ell$ decays with hadronic tagging at Belle*, arXiv:1702.01521 [INSPIRE].

[68] M. Tanaka and R. Watanabe, *Tau longitudinal polarization in $B \to D\tau\nu$ and its role in the search for charged Higgs boson*, *Phys. Rev.* **D 82** (2010) 034027 [arXiv:1005.4306] [INSPIRE].

[69] S. Descotes-Genon, J. Matias and J. Virto, *Understanding the $B \to K^*\mu^+\mu^-$ Anomaly*, *Phys. Rev.* **D 88** (2013) 074002 [arXiv:1307.5683] [INSPIRE].

[70] G. Hiller and M. Schmaltz, *R_K and future $b \to s\ell\ell$ physics beyond the standard model opportunities*, *Phys. Rev.* **D 90** (2014) 054014 [arXiv:1408.1627] [INSPIRE].

[71] W. Altmannshofer and D.M. Straub, *Implications of $b \to s$ measurements*, in proceedings of *50th Rencontres de Moriond Electroweak Interactions and Unified Theories*, La Thuile, Italy, March 14–21, 2015, pp. 333–338 [arXiv:1503.06199] [INSPIRE].

[72] S. Descotes-Genon, L. Hofer, J. Matias and J. Virto, *Global analysis of $b \to s\ell\ell$ anomalies*, *JHEP* **06** (2016) 092 [arXiv:1510.04239] [INSPIRE].

[73] T. Hurth, F. Mahmoudi and S. Neshatpour, *On the anomalies in the latest LHCb data*, *Nucl. Phys.* **B 909** (2016) 737 [arXiv:1603.00865] [INSPIRE].

[74] W. Altmannshofer, P. Stangl and D.M. Straub, *Interpreting Hints for Lepton Flavor Universality Violation*, *Phys. Rev.* **D 96** (2017) 055008 [arXiv:1704.05435] [INSPIRE].

[75] G. D'Amico et al., *Flavour anomalies after the R_{K^*} measurement*, *JHEP* **09** (2017) 010 [arXiv:1704.05438] [INSPIRE].

[76] M. Ciuchini et al., *On Flavourful Easter eggs for New Physics hunger and Lepton Flavour Universality violation*, *Eur. Phys. J.* **C 77** (2017) 688 [arXiv:1704.05447] [INSPIRE].

JHEP05(2018)173

[77] D. Bardhan, P. Byakti and D. Ghosh, *Role of Tensor operators in R_K and R_{K^*}*, *Phys. Lett.* **B 773** (2017) 505 [arXiv:1705.09305] [INSPIRE].

[78] LHCb collaboration, *Measurement of the $B_s^0 \to \mu^+\mu^-$ branching fraction and effective lifetime and search for $B^0 \to \mu^+\mu^-$ decays*, *Phys. Rev. Lett.* **118** (2017) 191801 [arXiv:1703.05747] [INSPIRE].

[79] K. Hagiwara, R. Liao, A.D. Martin, D. Nomura and T. Teubner, *$(g-2)_\mu$ and $\alpha(M_Z^2)$ re-evaluated using new precise data*, *J. Phys.* **G 38** (2011) 085003 [arXiv:1105.3149] [INSPIRE].

[80] M. Davier, *Update of the Hadronic Vacuum Polarisation Contribution to the muon $g-2$*, *Nucl. Part. Phys. Proc.* **287-288** (2017) 70 [arXiv:1612.02743] [INSPIRE].

[81] F. Jegerlehner, *Muon $g-2$ theory: The hadronic part*, *EPJ Web Conf.* **166** (2018) 00022 [arXiv:1705.00263] [INSPIRE].

[82] K. Hagiwara, A. Keshavarzi, A.D. Martin, D. Nomura and T. Teubner, *g-2 of the muon: status report*, *Nucl. Part. Phys. Proc.* **287-288** (2017) 33 [INSPIRE].

[83] A. Celis, J. Fuentes-Martin, A. Vicente and J. Virto, *Gauge-invariant implications of the LHCb measurements on lepton-flavor nonuniversality*, *Phys. Rev.* **D 96** (2017) 035026 [arXiv:1704.05672] [INSPIRE].

[84] PLANCK collaboration, P.A.R. Ade et al., *Planck 2013 results. XVI. Cosmological parameters*, *Astron. Astrophys.* **571** (2014) A16 [arXiv:1303.5076] [INSPIRE].

[85] S.M. Davidson and H.E. Logan, *Dirac neutrinos from a second Higgs doublet*, *Phys. Rev.* **D 80** (2009) 095008 [arXiv:0906.3335] [INSPIRE].

[86] J. Kawamura, S. Okawa and Y. Omura, *Interplay between the $b \to s\ell\ell$ anomalies and dark matter physics*, *Phys. Rev.* **D 96** (2017) 075041 [arXiv:1706.04344] [INSPIRE].

[87] P. Asadi, M.R. Buckley and D. Shih, *It's all right(-handed neutrinos): a new W' model for the $R_{D^{(*)}}$ anomaly*, arXiv:1804.04135 [INSPIRE].

[88] A. Greljo, D.J. Robinson, B. Shakya and J. Zupan, *$R(D^{(*)})$ from W' and right-handed neutrinos*, arXiv:1804.04642 [INSPIRE].

[89] R.W. Brown, R.H. Hobbs, J. Smith and N. Stanko, *Intermediate boson. iii. virtual-boson effects in neutrino trident production*, *Phys. Rev.* **D 6** (1972) 3273 [INSPIRE].

[90] W. Altmannshofer, S. Gori, M. Pospelov and I. Yavin, *Neutrino Trident Production: A Powerful Probe of New Physics with Neutrino Beams*, *Phys. Rev. Lett.* **113** (2014) 091801 [arXiv:1406.2332] [INSPIRE].

[91] D. Atwood, S.K. Gupta and A. Soni, *Same-sign Tops: A Powerful Diagnostic Test for Models of New Physics*, *JHEP* **04** (2013) 035 [arXiv:1301.2250] [INSPIRE].

[92] R. Goldouzian, *Search for top quark flavor changing neutral currents in same-sign top quark production*, *Phys. Rev.* **D 91** (2015) 014022 [arXiv:1408.0493] [INSPIRE].

[93] N. Craig, F. D'Eramo, P. Draper, S. Thomas and H. Zhang, *The Hunt for the Rest of the Higgs Bosons*, *JHEP* **06** (2015) 137 [arXiv:1504.04630] [INSPIRE].

[94] C.-W. Chiang, H. Fukuda, M. Takeuchi and T.T. Yanagida, *Flavor-Changing Neutral-Current Decays in Top-Specific Variant Axion Model*, *JHEP* **11** (2015) 057 [arXiv:1507.04354] [INSPIRE].

JHEP05(2018)173

[95] C.S. Kim, Y.W. Yoon and X.-B. Yuan, *Exploring top quark FCNC within 2HDM type-III in association with flavor physics*, *JHEP* **12** (2015) 038 [arXiv:1509.00491] [INSPIRE].

[96] S. Gori, I.-W. Kim, N.R. Shah and K.M. Zurek, *Closing the Wedge: Search Strategies for Extended Higgs Sectors with Heavy Flavor Final States*, *Phys. Rev.* **D 93** (2016) 075038 [arXiv:1602.02782] [INSPIRE].

[97] R. Patrick, P. Sharma and A.G. Williams, *Exploring a heavy charged Higgs using jet substructure in a fully hadronic channel*, *Nucl. Phys.* **B 917** (2017) 19 [arXiv:1610.05917] [INSPIRE].

[98] W. Altmannshofer, P. Bhupal Dev and A. Soni, $R_{D^{(*)}}$ *anomaly: A possible hint for natural supersymmetry with R-parity violation*, *Phys. Rev.* **D 96** (2017) 095010 [arXiv:1704.06659] [INSPIRE].

[99] M.D. Campos, D. Cogollo, M. Lindner, T. Melo, F.S. Queiroz and W. Rodejohann, *Neutrino Masses and Absence of Flavor Changing Interactions in the 2HDM from Gauge Principles*, *JHEP* **08** (2017) 092 [arXiv:1705.05388] [INSPIRE].

[100] S. Gori, C. Grojean, A. Juste and A. Paul, *Heavy Higgs Searches: Flavour Matters*, *JHEP* **01** (2018) 108 [arXiv:1710.03752] [INSPIRE].

[101] M. Kohda, T. Modak and W.-S. Hou, *Searching for new scalar bosons via triple-top signature in* $cg \to tS^0 \to tt\bar{t}$, *Phys. Lett.* **B 776** (2018) 379 [arXiv:1710.07260] [INSPIRE].

[102] R. Patrick, P. Sharma and A.G. Williams, *Triple top signal as a probe of charged Higgs in a 2HDM*, *Phys. Lett.* **B 780** (2018) 603 [arXiv:1710.08086] [INSPIRE].

[103] A. Arhrib, R. Benbrik, S. Moretti, R. Santos and P. Sharma, *Signal to background interference in* $pp \to tH^- \to tW^-b\bar{b}$ *at the LHC Run-II*, *Phys. Rev.* **D 97** (2018) 075037 [arXiv:1712.05018] [INSPIRE].

[104] A. Belyaev, N.D. Christensen and A. Pukhov, *CalcHEP 3.4 for collider physics within and beyond the Standard Model*, *Comput. Phys. Commun.* **184** (2013) 1729 [arXiv:1207.6082] [INSPIRE].

[105] ATLAS collaboration, *Search for a new heavy gauge boson resonance decaying into a lepton and missing transverse momentum in* $36\,fb^{-1}$ *of pp collisions at* $\sqrt{s} = 13$ *TeV with the ATLAS experiment*, arXiv:1706.04786 [INSPIRE].

[106] ATLAS collaboration, *Search for High-Mass Resonances Decaying to* $\tau\nu$ *in pp Collisions at* $\sqrt{s} = 13$ *TeV with the ATLAS Detector*, *Phys. Rev. Lett.* **120** (2018) 161802 [arXiv:1801.06992] [INSPIRE].

[107] CMS collaboration, *Search for W' decaying to tau lepton and neutrino in proton-proton collisions at* $\sqrt{s} = 8$ *TeV*, *Phys. Lett.* **B 755** (2016) 196 [arXiv:1508.04308] [INSPIRE].

[108] CMS collaboration, *Search for W' decaying to tau lepton and neutrino in proton-proton collisions at* $\sqrt{s} = 13$ *TeV*, CMS-PAS-EXO-16-006.

[109] ATLAS collaboration, *Search for invisible particles produced in association with single-top-quarks in proton-proton collisions at* $\sqrt{s} = 8$ *TeV with the ATLAS detector*, *Eur. Phys. J.* **C 75** (2015) 79 [arXiv:1410.5404] [INSPIRE].

[110] CMS collaboration, *Search for Monotop Signatures in Proton-Proton Collisions at* $\sqrt{s} =$ *8 TeV*, *Phys. Rev. Lett.* **114** (2015) 101801 [arXiv:1410.1149] [INSPIRE].

JHEP05(2018)173

[111] CMS collaboration, *Search for physics beyond the standard model in events with two leptons of same sign, missing transverse momentum and jets in proton-proton collisions at* $\sqrt{s} = 13$ *TeV*, *Eur. Phys. J.* **C 77** (2017) 578 [arXiv:1704.07323] [INSPIRE].

[112] FERMILAB LATTICE, MILC collaborations, A. Bazavov et al., $B^0_{(s)}$*-mixing matrix elements from lattice QCD for the Standard Model and beyond*, *Phys. Rev.* **D 93** (2016) 113016 [arXiv:1602.03560] [INSPIRE].

[113] HPQCD collaboration, R.J. Dowdall, C.T.H. Davies, R.R. Horgan, C.J. Monahan and J. Shigemitsu, *B-Meson Decay Constants from Improved Lattice Nonrelativistic QCD with Physical u, d, s and c Quarks*, *Phys. Rev. Lett.* **110** (2013) 222003 [arXiv:1302.2644] [INSPIRE].

[114] HPQCD collaboration, B. Colquhoun et al., *B-meson decay constants: a more complete picture from full lattice QCD*, *Phys. Rev.* **D 91** (2015) 114509 [arXiv:1503.05762] [INSPIRE].

[115] FERMILAB LATTICE, MILC collaborations, J.A. Bailey et al., *Update of* $|V_{cb}|$ *from the* $\bar{B} \to D^* \ell \bar{\nu}$ *form factor at zero recoil with three-flavor lattice QCD*, *Phys. Rev.* **D 89** (2014) 114504 [arXiv:1403.0635] [INSPIRE].

[116] M. Okamoto et al., *Semileptonic* $D \to \pi/K$ *and* $B \to \pi/D$ *decays in* $2+1$ *flavor lattice QCD*, *Nucl. Phys. Proc. Suppl.* **140** (2005) 461 [hep-lat/0409116] [INSPIRE].

JHEP05(2018)173